





Cancellation of one-parameter graviton gauge dependence in the effective scalar field equation in de Sitter

Dražen Glavan ^{a,*} Shun-Pei Miao ^{b,†} Tomislav Prokopec ^{c,‡} Richard P. Woodard ^{d,§}

^a *CEICO, Institute of Physics of the Czech Academy of Sciences (FZU),
Na Slovance 1992/2, 182 21 Prague 8, Czech Republic*

^b *Department of Physics, National Cheng Kung University,
No. 1 University Road, Tainan City, 70101, Taiwan*

^c *Institute for Theoretical Physics, Spinoza Institute & EMMEΦ, Utrecht University,
Postbus 80.195, 3508 TD Utrecht, The Netherlands*

^d *Department of Physics, University of Florida, Gainesville, FL 32611, U.S.A.*

We investigate gauge dependence of one-graviton-loop corrections to the effective field equation of the massless, minimally coupled scalar in de Sitter, obtained by including source and observer corrections to the effective self-mass correcting the equation. Using the $\Delta\alpha$ variation of the de Sitter-breaking graviton propagator in a one-parameter family of gauges, we compute the gauge-dependent contributions to the effective self-mass of a massless minimally coupled scalar mediating interactions between heavy scalars. We show that gauge dependence cancels provided the contributions from all diagram classes are collected, including one-loop corrections to external mode functions, which play a qualitatively new role relative to flat space. The resulting cancellation supports the construction of graviton gauge-independent cosmological quantum-gravitational observables from quantum-corrected effective equations.

Contents

1	Introduction	2
2	The problem and the goal	5
3	Reduction strategy	7
3.1	General reduction	7
3.2	One-loop reduction	9
4	Feynman diagrams	10
4.1	One-loop diagrams for 4-point functions	12
4.2	Consolidated one-loop diagrams for the 4-point function	14
4.3	One-loop diagrams for mode function corrections	16

*email: glavan@fzu.cz

†email: spmiao5@mail.ncku.edu.tw

‡email: t.prokopec@uu.nl

§email: woodard@phys.ufl.edu

5	Propagators	17
6	Reducing 4-point diagrams	19
6.1	Preliminary reduction of AA parts	19
6.2	Preliminary reduction of BB parts	24
6.3	Final reduction	27
7	Reducing mode function corrections	28
7.1	Preliminary reduction of AA parts	28
7.2	Preliminary reduction of BB parts	29
7.3	Final reduction	30
7.4	Contribution to effective self-mass	31
8	Discussion and conclusions	32
	Acknowledgments	34
A	Integrated propagators	34
B	Additional diagrams	35

1 Introduction

The rapid accelerated expansion of space during primordial inflation provides conditions for efficient gravitational particle production [1], experienced by fields non-conformally coupled to gravity. It is by this linear quantum field-theoretic mechanism that inflation produces a vast ensemble of long-wavelength scalar [2] and tensor [3] cosmological perturbations, i.e. inflationary scalars and gravitons, respectively. These inflationary quanta—more precisely, the remnants they leave on the cosmic microwave background—have become the main probes of inflationary physics [4].

It should be noted that gravity couples universally, and that the vast ensemble of inflationary gravitons in principle must interact with all matter fields, and also with itself. In addition, the relatively high energy scale of inflation, potentially as high as the GUT scale of 10^{16} GeV, opens the possibility of inflationary quantum-gravitational effects that are not prohibitively small, while still being describable by the effective field theory of gravity [5–10]. Moreover, gravitons can mediate the effects of the rapid expansion to conformally coupled fields (such as electromagnetism), thereby breaking conformal invariance and potentially leaving observable imprints. Investigating this possibility is of our primary interest.

The naive dimensional-analysis estimate for the size of quantum-gravitational effects during inflation is $\kappa^2 H^2 \sim 10^{-11}–10^{-10}$, where H is the almost-constant inflationary Hubble rate, and $\kappa = \sqrt{16\pi G_N}$ is the loop-counting parameter of quantum gravity. However, explicit computations have shown that these corrections can be enhanced by large logarithms, either temporal or spatial. These computations are performed in rigid de Sitter space with constant Hubble rate, which is a good approximation for the purpose at hand and offers considerable technical simplifications. Thus far, six systems that exhibit logarithmic enhancement of loop corrections have been identified:¹

¹Temporal growth of the dynamical massless, conformally coupled scalar has also been reported [11], but this result did not persist after further scrutiny [12].

- Temporal growth of the dynamical fermion field strength [13];
- Temporal and spatial growth of the electric force [14];
- Temporal growth of the dynamical photon field strength [15];
- Temporal growth of the dynamical graviton field strength [16];
- Spatial suppression of the force mediated by a massless minimally coupled scalar [17];
- Temporal suppression of the gravitational force [18].

The origin of large secular logarithms can be explained by a combination of stochastic formalism and renormalization group [19, 20].

However, a serious question pertains to these results: the *gauge issue*. All results above have been worked out in the simplest graviton gauge [21, 22]. The procedure was to compute the one-graviton-loop correction to the relevant 1-particle-irreducible (1PI) 2-point function (self-mass/self-energy/vacuum polarization) [23–28], and then use it to quantum-correct the effective field equations. The concern is that this procedure need not yield gauge-independent physical predictions, in particular for the logarithmically enhanced terms, and the explicit computations [13–18] have been criticized on that account [29–32].

A computation of the graviton loop correction to dynamical photons performed in the one-parameter family of exact covariant gauges [33] brings this issue into focus. The vacuum polarization computed in this gauge [34] has been used to infer the correction to the field strength of a dynamical photon [35]. This correction does not depend on the gauge-fixing parameter of the exact covariant gauge and does show secular enhancement, but its amplitude differs from the noncovariant gauge computation [15]. This underscores the need to address the *gauge issue* of quantum-gravitational loop corrections in cosmological quantum field theory, i.e. to purge gauge dependence from physical observables. In this work we report progress toward this goal by testing the de Sitter generalization of the proposal of [36], designed to produce gauge-independent one-loop-corrected effective field equations, by including the analogues of source and observer corrections to self-masses.

The gauge dependence of 1PI two-point functions is well established in flat space, and using them directly to quantum-correct field equations is not in general the correct procedure for extracting physical gauge-independent predictions (see e.g. [37]). In flat space this problem is solved for asymptotic particle scattering by the construction of the S-matrix, in gauge theories and in quantum gravity. In curved space the S-matrix does not generally exist because of the absence of asymptotic states, and in any case cosmological applications are inherently initial-value problems. This motivates constructing appropriate one-loop quantum-gravitational observables for inflation.

One-graviton-loop corrections to 1PI two-point functions in de Sitter space must inherit at least the flat-space gauge dependence. The relevant question is how much of this gauge dependence contaminates the logarithmically enhanced terms, and how to purge it. In flat space the S-matrix achieves gauge independence by accounting for source and observer corrections to the scattering process. One can apply inverse-scattering methods to the S-matrix in order to infer quantum-corrected long-range potentials [5, 38–40]. Moreover, the relevant long-range contributions can be isolated more directly by analyzing the non-analytic behaviour of momentum-space amplitudes.

The S-matrix achieves gauge-independence by putting the amputated connected n -point functions on shell by attaching to them asymptotic mode functions. In flat space this form is obtained by the Lehmann–Symanzik–Zimmermann (LSZ) reduction formula [41]. A generalization of this procedure was proposed in [36] that dispenses with taking asymptotic time limits,

allowing generalizations to curved spacetimes.² In particular, one considers an amputated 4-point function in position space and puts it on shell by attaching mode functions at finite time. This object includes source and observer corrections much like the S-matrix. One then employs integration by parts, and the Donoghue Identities [38–40, 45] to reduce the one-loop diagrams to the topology of the self-mass diagram, from which the effective gauge-independent self-mass can be read off. This effective self-mass can then be used to quantum-correct effective field equations, thus purging gauge dependence from them. This program has been demonstrated to work for long-range corrections to potentials in flat space for the scalar model [36], and for electromagnetism [46], and here we investigate whether gauge independence is maintained in its de Sitter space generalization.

In this work we report on the computation of all the diagrams contributing to the gauge-independent effective self-mass by using the gauge-dependent part of the graviton propagator in the simple one-parameter gauge [47, 48], that we refer to as the $\Delta\alpha$ variation of the graviton propagator. We demonstrate that the gauge dependence drops out from the final answer by showing that all contributions from the $\Delta\alpha$ variation sum to zero. Thus, in principle, we establish the gauge independence of the entire construction. Furthermore, we find that the previous computation [49], that we performed using the simplest gauge graviton propagator [21, 22] corresponding to $\Delta\alpha=0$, should be supplemented by contributions from additional diagrams we identify here in order to yield the full gauge-independent result.

We find that no Donoghue Identities are necessary for the present computation. On the one hand, this does not allow us to test the de Sitter versions of the Donoghue Identities used in [49]. On the other hand, it allows an unambiguous test of which diagrams and contributions must be included to ensure gauge independence. We find that, unlike in flat space, additional diagrams and contributions are necessary, including the one-loop corrections to the external mode functions, that are crucial for obtaining gauge independence. This is not seen in flat space, where such corrections can at most be absorbed into a constant multiplicative field-strength. In curved space, secular corrections to mode functions are possible; they combine with one-loop corrections to the amputated four-point function to yield a gauge-independent result.

We should also mention the approach to eliminate gauge dependence by taking the expectation values of gauge invariant operators. This is straightforward for linearized gravity, and was accomplished long ago for cosmological perturbations [50]. However, it is quite nontrivial when interactions are included because one must invariantly fix the points at which observations are made and the frames in which any tensor indices are reported [51–61]. Devising a reasonable way of accomplishing this is crucial because there is no local way to specify the coordinate system and frame fields [62], but permitting arbitrary nonlocal additions to the operator under study allows one to completely cancel any correction to the linearized operator from interaction vertices [63], including what are known to be real effects in flat space scattering. The problem has both a technical and a physical aspect. On the technical level, nonlinear additions to the operator under study inevitably involve new sorts of divergences [51, 64, 65], which are not removed by the BPHZ (Bogoliubov and Parasiuk [66], Hepp [67] and Zimmermann [68, 69]) renormalizations that suffice for noncoincident 1PI n -point functions. Removing these divergences requires the more complicated procedure of composite operator renormalization [70–72]. The physics issue is that the finite residues of the new divergences can change scaling and renormalization group flows. For example, flat space scattering amplitudes defined using invariant Green’s functions at fixed geodesic separations produce an extra high energy logarithm at one loop order [65].

The paper is organized as follows. Section 2 outlines in more detail the main problem we address and the goal of constructing gauge-independent observables. Section 3 gives the general strategy for the reduction to self-mass diagrams. Section 4 lists the Feynman rules for the model

²Although the S-matrix does exist for massive scalars on de Sitter [42] (see also [43, 44]), the construction is likely problematic for massless, minimally coupled scalars and gravitons precisely because of the secular growth that makes these fields so interesting.

and all classes of diagrams necessary for the computation, including simplifications obtained by consolidating some classes. Section 5 collects the relevant properties of scalar and graviton propagators. The main computation is presented in Sections 6 and 7, where contributions from the four-point diagrams and from mode-function corrections are presented, respectively. The concluding Section 8 collects all contributions to show that they cancel and provides a discussion. Mathematical details and the discussion of additional diagrams are relegated to the appendices.

2 The problem and the goal

In order to investigate the problem of gauge dependence of the quantum-gravitationally-corrected effective field equations in de Sitter space, we consider a specific minimal model where explicit computations are tractable. We consider a massive scalar Ψ with $m \gg H$, interacting via the massless, minimally coupled (MMC) scalar φ in de Sitter space. The covariant action that describes this system is given by

$$S[g_{\mu\nu}, \varphi, \Psi] = \int d^Dx \sqrt{-g} \left[\frac{R - (D-2)\Lambda}{\kappa^2} - \frac{1}{2}g^{\mu\nu}(\partial_\mu\varphi)(\partial_\nu\varphi) - \frac{1}{2}g^{\mu\nu}(\partial_\mu\Psi)(\partial_\nu\Psi) - \frac{1}{2}(m^2 + \lambda\varphi)\Psi^2 \right], \quad (2.1)$$

where $\kappa^2 = 16\pi G$ is the rescaled Newton constant, Λ is the positive cosmological constant, R is the Ricci scalar,³ and λ is a dimensionful coupling constant.

We are interested in investigating this two-scalar system on a spatially-flat de Sitter space background, for which the metric is conformal to the Minkowski one, $g_{\mu\nu} = a^2(\eta)\eta_{\mu\nu}$, when written in conformal time coordinate η that takes values on a negative semi-axis, $-\infty < \eta < 0$. The scale factor of de Sitter space grows with conformal time, $a(\eta) = -1/(H\eta)$, while the Hubble rate remains constant, $H = \sqrt{\Lambda/3}$. In particular, we are interested in one-graviton loop corrections to the interaction between heavy scalars Ψ that is mediated by the MMC scalar φ . In this setup the fluctuations of the metric field, that we define as

$$g_{\mu\nu} = a^2(\eta_{\mu\nu} + \kappa h_{\mu\nu}), \quad (2.2)$$

are quantized semiclassically, and the effects of their interactions are captured by perturbative quantum field theory. The interaction vertices encoded in the action (2.1) that we will need for our computation are collected in Table 1. In the remainder of this section we outline what is the problem that arises in the study of quantum-gravitational corrections to the system defined in (2.1), while the following section is devoted to the outline of our strategy for addressing this problem.

The MMC scalar interacting with inflationary gravitons is the simplest system in de Sitter space that exhibits a large secular logarithm in the one graviton loop correction [17]. The tree-level point-source potential mediated by the MMC scalar is given by [73, 74]

$$\varphi_0(r) = -\frac{K}{4\pi ar} - \frac{KH}{4\pi} \ln\left[\frac{a}{1+aHr}\right] \xrightarrow{aHr \gg 1} \frac{KH}{4\pi} \ln(Hr). \quad (2.3)$$

The first term in the middle equality is just the de Sitter generalization of the flat space potential, while the second tail term, dominant for large physical distances, is the pure de Sitter space contribution. The tree-level potential in (2.3) is a solution to the classical field equation with a point source,

$$\mathcal{D}\varphi(x) = Ka\delta^3(\vec{x}), \quad (2.4)$$

³Our conventions are $\eta_{\mu\nu} = (-1, 1, \dots, 1)$ for the Minkowski metric, and $R_{\mu\nu} = \partial_\alpha\Gamma_{\mu\nu}^\alpha - \partial_\nu\Gamma_{\mu\alpha}^\alpha + \Gamma_{\mu\nu}^\alpha\Gamma_{\beta\alpha}^\beta - \Gamma_{\mu\beta}^\alpha\Gamma_{\nu\alpha}^\beta$ for the Ricci tensor.

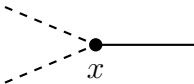
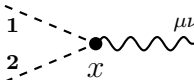
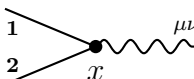

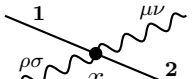


A		$-i\lambda a_x^D$
B		$-i\kappa a_x^{D-2} \left[-\partial_1^{(\mu} \partial_2^{\nu)} + \frac{1}{2} \eta^{\mu\nu} (\partial_1 \cdot \partial_2 + a_x^2 m^2) \right]$
C		$-i\kappa a_x^{D-2} \left[-\partial_1^{(\mu} \partial_2^{\nu)} + \frac{1}{2} \eta^{\mu\nu} \partial_1 \cdot \partial_2 \right]$
D		$-\frac{1}{2} i\kappa \lambda a_x^D \eta^{\mu\nu}$
E		$-i\kappa^2 a_x^{D-2} \left[\frac{1}{2} \partial_1^{(\mu} \eta^{\nu)(\rho} \partial_2^{\sigma)} + \frac{1}{2} \partial_1^{(\rho} \eta^{\sigma)(\mu} \partial_2^{\nu)} - \frac{1}{4} \partial_1^{(\mu} \partial_2^{\nu)} \eta^{\rho\sigma} - \frac{1}{4} \partial_1^{(\rho} \partial_2^{\sigma)} \eta^{\mu\nu} \right. \\ \left. - \frac{1}{8} (2\eta^{\mu(\rho} \eta^{\sigma)\nu} - \eta^{\mu\nu} \eta^{\rho\sigma}) \partial_1 \cdot \partial_2 \right]$
F		$-i\kappa^2 a_x^{D-2} \left[\frac{1}{2} \partial_1^{(\mu} \eta^{\nu)(\rho} \partial_2^{\sigma)} + \frac{1}{2} \partial_1^{(\rho} \eta^{\sigma)(\mu} \partial_2^{\nu)} - \frac{1}{4} \partial_1^{(\mu} \partial_2^{\nu)} \eta^{\rho\sigma} - \frac{1}{4} \partial_1^{(\rho} \partial_2^{\sigma)} \eta^{\mu\nu} \right. \\ \left. - \frac{1}{8} (2\eta^{\mu(\rho} \eta^{\sigma)\nu} - \eta^{\mu\nu} \eta^{\rho\sigma}) (\partial_1 \cdot \partial_2 + a_x^2 m^2) \right]$
G		$-i\kappa^2 \lambda a_x^D \left[\frac{1}{8} \eta^{\mu\nu} \eta^{\rho\sigma} - \frac{1}{4} \eta^{\mu(\rho} \eta^{\sigma)\nu} \right]$

Table 1: List of 3-point, 4-point, and 5-point interaction vertices encoded in the action (2.1), that are relevant for the computation of the one-graviton-loop correction to the scalar exchange potential. Solid lines correspond to the MMC scalar, dashed lines to the massive scalar, and wavy lines to the graviton.

where $\mathcal{D} = \partial^\mu a^{D-2} \partial_\mu$, and K is the scalar charge of the point particle.

The long-range interaction in (2.3) receives quantum gravitational corrections from interactions with an ensemble of inflationary gravitons. These corrections are inferred by computing the one-loop MMC scalar self-mass, $-i\mathcal{M}^2$, with a single graviton running in the loop, and using it to correct the classical equation of motion (2.4),

$$\mathcal{D}\varphi(x) - \int d^4x' \mathcal{M}^2(x; x') \varphi(x') = K a \delta^3(\vec{x}). \quad (2.5)$$

Of course, it is the retarded self-mass component obtained in the Schwinger-Keldysh formalism for nonequilibrium quantum field theory [75–82] that corrects this equation. This self-mass has been computed in the simple graviton gauge [17], and leads to the following result for the one-loop corrected potential

$$\varphi(x) \xrightarrow{aHr \gg 1} \varphi_0(r) \times \left[1 - \frac{\kappa^2 H^2}{8\pi^2} \ln(Hr) \right], \quad (2.6)$$

that exhibits a large suppression of the tree-level potential for large physical distances.

The one-loop quantum gravitational correction in (2.6) enhanced by the spatially-dependent logarithm is exciting, as it signals effects considerably larger than expected by naive dimensional analysis. However, it is not clear that (2.6) is the full physical result, or whether a part of it is a gauge artifact. This is because the self-mass used to quantum correct the field equation (2.5) is known to be a gauge-dependent object. This gauge dependence is not manifest because the

result was obtained in a gauge without free gauge parameters, but we know that at least the flat space gauge dependence must survive the de Sitter generalization. For this reason, the main objective of our program is purging gauge dependence from 1PI 2-point functions that correct the field equations, in particular here from the MMC scalar self-mass.

Our intention is to construct an effective gauge-independent self-mass $-i\mathcal{M}^2(x; x')$, that can be used to correct the field equation (2.4). In order to accomplish this, we appeal to the lessons from the flat space inverse scattering method, where the long-range potential can be extracted from the t -channel $2 \rightarrow 2$ scattering of massive source and observer particles. The quantum-field-theoretic object corresponding to this process is the t -channel amputated 4-point function of the massive scalar, that is put on shell by attaching the asymptotic plane-wave mode functions.

We propose to consider the analogous object in de Sitter space, with the massive scalar Ψ playing the same role of source and observer, and consider its amputated 4-point function that is now put on shell at finite times, by attaching mode functions that themselves satisfy quantum corrected equations of motion. It is possible to reduce all one-loop diagrams contributing to this object to the topology of the t -channel self-mass diagram, put on shell by the tree-level mode functions. This self-mass should capture the infrared effects that are behind large logarithms in de Sitter space corrections. We then read off this effective self-mass and use it to quantum correct the field equations as in (2.5). We conjecture that this effective self-mass should be gauge-independent, and this work is devoted to showing the independence on one of the two gauge-fixing parameters of the graviton propagator in the tractable non-covariant gauge [47, 48]. The general reduction procedure we follow to extract the one-loop effective self-mass is outlined in the following section.

3 Reduction strategy

3.1 General reduction

Our starting point is the amputated connected four-point function for the massive scalar field Ψ . We put this object on shell by attaching to it mode functions $U(x)$ of the massive scalar field,

$$\begin{array}{c} \text{---} \circ U^* \text{---} \\ \diagup \quad \diagdown \\ \text{---} \circ U^* \text{---} \\ \diagdown \quad \diagup \\ \text{---} \circ U \text{---} \\ \diagup \quad \diagdown \\ \text{---} \circ U \text{---} \end{array} \equiv \int d^D x U(x) \int d^D y U^*(y) \int d^D x' U(x') \int d^D y' U^*(y') \left(\begin{array}{c} \text{---} \circ U^* \text{---} \\ \diagup \quad \diagdown \\ \text{---} \circ U^* \text{---} \\ \diagdown \quad \diagup \\ \text{---} \circ U \text{---} \\ \diagup \quad \diagdown \\ \text{---} \circ U \text{---} \end{array} \right). \quad (3.1)$$

It is crucial that the attached mode functions satisfy the quantum-corrected equation of motion,

$$(\mathcal{D}_x - a_x^D m^2)U(x) - \int d^4 x' \mathcal{M}_m^2(x; x')U(x') = 0, \quad (3.2)$$

where $-i\mathcal{M}_m^2$ is the self-mass of the massive scalar field Ψ . In the limit of flat space, and upon specializing the mode functions to asymptotic plane waves, this expression reduces to the LSZ reduction formula that is known to yield the gauge-independent S-matrix. We find (3.1) to be the appropriate curved space generalization of the LSZ reduction formula, and in this work we show its gauge independence.

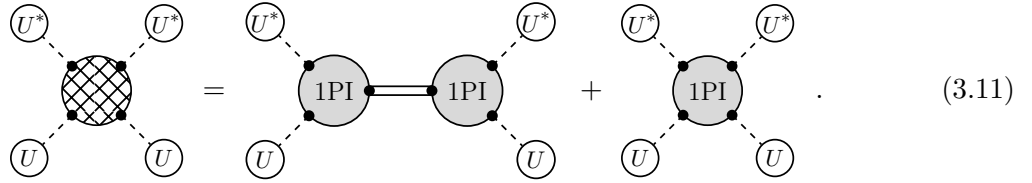
The ultimate goal is to capture the physical part of the large logarithms in graviton loop corrections in de Sitter space, by isolating the gauge-independent part of the scalar self-mass. To this end we reduce the diagrams contributing to (3.1) to the following form in the limit $m/H \gg 1$,

$$\begin{array}{c} \text{---} \circ U^* \text{---} \\ \diagup \quad \diagdown \\ \text{---} \circ U^* \text{---} \\ \diagdown \quad \diagup \\ \text{---} \circ U \text{---} \\ \diagup \quad \diagdown \\ \text{---} \circ U \text{---} \end{array} \longrightarrow \begin{array}{c} \text{---} \circ u^* \text{---} \\ \diagup \quad \diagdown \\ \text{---} \circ u^* \text{---} \\ \diagdown \quad \diagup \\ \text{---} \circ u \text{---} \\ \diagup \quad \diagdown \\ \text{---} \circ u \text{---} \end{array} + \begin{array}{c} \text{---} \circ u^* \text{---} \\ \diagup \quad \diagdown \\ \text{---} \circ u^* \text{---} \\ \diagdown \quad \diagup \\ \text{---} \circ u \text{---} \\ \diagup \quad \diagdown \\ \text{---} \circ u \text{---} \end{array} + \begin{array}{c} \text{---} \circ u^* \text{---} \\ \diagup \quad \diagdown \\ \text{---} \circ u^* \text{---} \\ \diagdown \quad \diagup \\ \text{---} \circ u \text{---} \\ \diagup \quad \diagdown \\ \text{---} \circ u \text{---} \end{array} + \begin{array}{c} \text{---} \circ u^* \text{---} \\ \diagup \quad \diagdown \\ \text{---} \circ u^* \text{---} \\ \diagdown \quad \diagup \\ \text{---} \circ u \text{---} \\ \diagup \quad \diagdown \\ \text{---} \circ u \text{---} \end{array} + \begin{array}{c} \text{---} \circ u^* \text{---} \\ \diagup \quad \diagdown \\ \text{---} \circ u^* \text{---} \\ \diagdown \quad \diagup \\ \text{---} \circ u \text{---} \\ \diagup \quad \diagdown \\ \text{---} \circ u \text{---} \end{array} \quad (3.3)$$

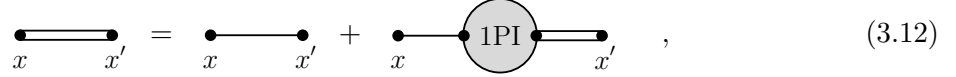
3.2 One-loop reduction

Applying the outlined procedure at one-loop level in flat space is straightforward [36]. It requires accounting for 6 classes of nonvanishing diagrams contributing to the 1PI 4-point function. Derivative interactions, together with the position space Donoghue identities are sufficient to accomplish the task. However, in de Sitter space the situation complicates significantly. In our previous work we have identified additional 4-point diagrams that contribute in de Sitter, but which vanish in flat space. In fact, in this work we find that the situation is even more complicated: we need to consider *all* one-loop 4-point functions, *and* the one-loop corrections to the attached mode functions. Only after accounting for all these contributions do we get that gauge dependence cancels. It therefore behooves us to review the reduction formalism and recast it in the language appropriate for our applications, which we do in this subsection.

The amputated 4-point function is best written as a skeleton expansion in terms of 1PI n -point functions, and resummed two-point functions,



Here the resummed MMC scalar propagator, denoted by the double solid line, satisfies the Dyson-Schwinger equation



where the single-line term on the right-hand side corresponds to the tree-level propagator.

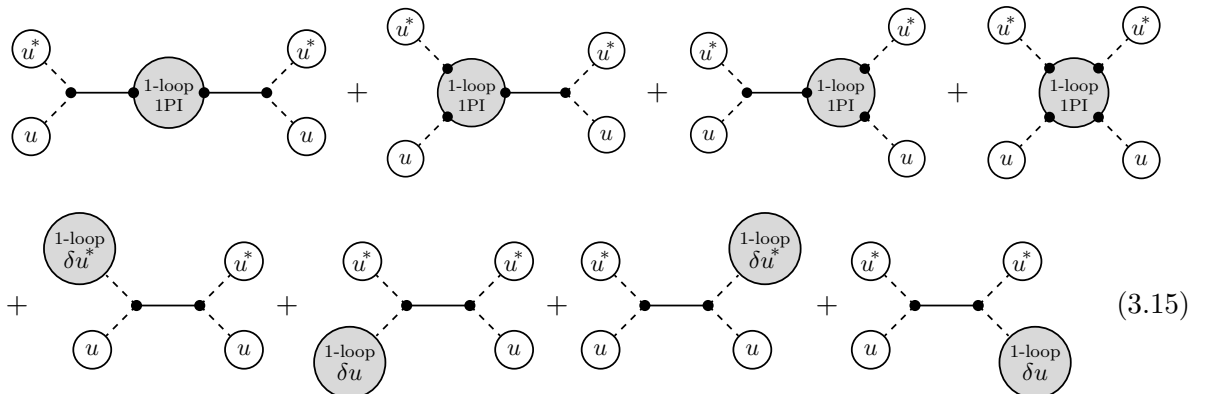
The diagram corresponding to the tree-level exchange potential (2.3) is



where the tree-level mode function u satisfies

$$(\mathcal{D}_x - a_x^D m^2)u(x) = 0. \quad (3.14)$$

The one-loop corrections to the exchange potential will be captured by the following diagrams:



The first diagram above descends from the first diagram on the right-hand side in (3.11) and comes from correcting the massless propagator by solving (3.12) to one-loop order. The two middle diagrams in the first line also descend from the first diagram in (3.11), by truncating the 1PI 3-vertex to one-loop order. Analogously, the last diagram in the first line above descends from the second diagram on the right-hand side in (3.11) by truncating the 1PI 4-vertex to one-loop order. On the other hand, all the diagrams of the second line above come from correcting the massive mode function, $U = u + \delta u$, by solving (3.2) for the one-loop correction,

$$(\mathcal{D}_x - a_x^D m^2) \delta u(x) = \int d^4 x' \mathcal{M}_m^2(x; x') u(x'), \quad (3.16)$$

where $\mathcal{M}_m^2(x; x')$ is the one-loop self-mass of the massive scalar.

4 Feynman diagrams

In this section we give expressions for all the relevant one-loop diagrams in the specific model given in (2.1). These diagrams are constructed from interaction vertices given in Table 1. The diagrams coming from the amputated 4-point function, corresponding to the first line in (3.15), are depicted in Fig. 1, while diagrams descending from the mode function corrections, corresponding to the second line in (3.15) are given in subsection 4.3 later on in the section.

We should comment on the form in which we give expressions corresponding to diagrams in Fig. 1. It is unnecessary to explicitly write some parts of diagrams that are common for all of them. For this reason we do not explicitly write the external mode functions, nor the integrals that attach them to the main part of the diagram. Instead, we give expressions for 4-point functions $-iV(x; y; x'; y')$ that are integrated over to obtain the diagrams,

$$(\text{Diag. } n) = \int d^D x u(x) \int d^D y u^*(y) \int d^D x' u(x') \int d^D y' u^*(y') \times \left[-iV_n(x; y; x'; y') \right], \quad (4.1)$$

where $n = 0, \dots, 7$. When manipulating the 4-point functions that appear in the integrand above, we immediately drop the terms from $-iV$ that annihilate the external mode function via its equation of motion (3.14).

We should also comment on the condensed notation for derivatives that we employ henceforth, that we find tremendously useful when performing computations. We found it very convenient to indicate where derivatives act by putting accents on them, rather than this being indicated by their placement. Given the preponderance of indices, this strategy saves a lot of time and effort, and makes for far more transparent expressions when one acclimates to reading it. Derivatives acting on the graviton propagator, or on the integrated propagators contained inside of it are always denoted by a tilde accent. Derivatives acting on either the scalar propagator in the loop, be it massive or massless, are denoted without accents, and derivatives acting on the scalar propagator outside the loop (again massive or massless) are denoted by a bar. There are some cases where these conventions lead to some ambiguity, which is removed by explicitly indicating the coordinate on the derivative, that can be matched with the corresponding vertex, and consequently the corresponding propagator. For example, the following expression

$$\begin{aligned} & \left\{ \partial_z^\mu i\Delta_A(x; z) \right\} \times \left\{ \partial_z^\nu i[\mu\nu\Delta_{\rho\sigma}](z; z') \right\} \times \left\{ \partial_z^\rho i\Delta_A(z; z') \right\} \times \left\{ \partial_z^\sigma i\Delta_A(z'; x') \right\} \\ & \longrightarrow \bar{\partial}_z^\mu \tilde{\partial}_z^\nu \partial_{z'}^\rho \bar{\partial}_{z'}^\sigma \times i\Delta_A(x; z) \left(\frac{i[\mu\nu\Delta_{\rho\sigma}](z; z')}{i\Delta_A(z; z')} \right) i\Delta_A(z'; x'). \end{aligned} \quad (4.2)$$

Furthermore, wherever possible, we try to write propagators in the loops in parentheses in order to visually resemble the diagram itself. In places where we unpack the condensed notation this is usually mentioned explicitly, and otherwise should be clear from the context.

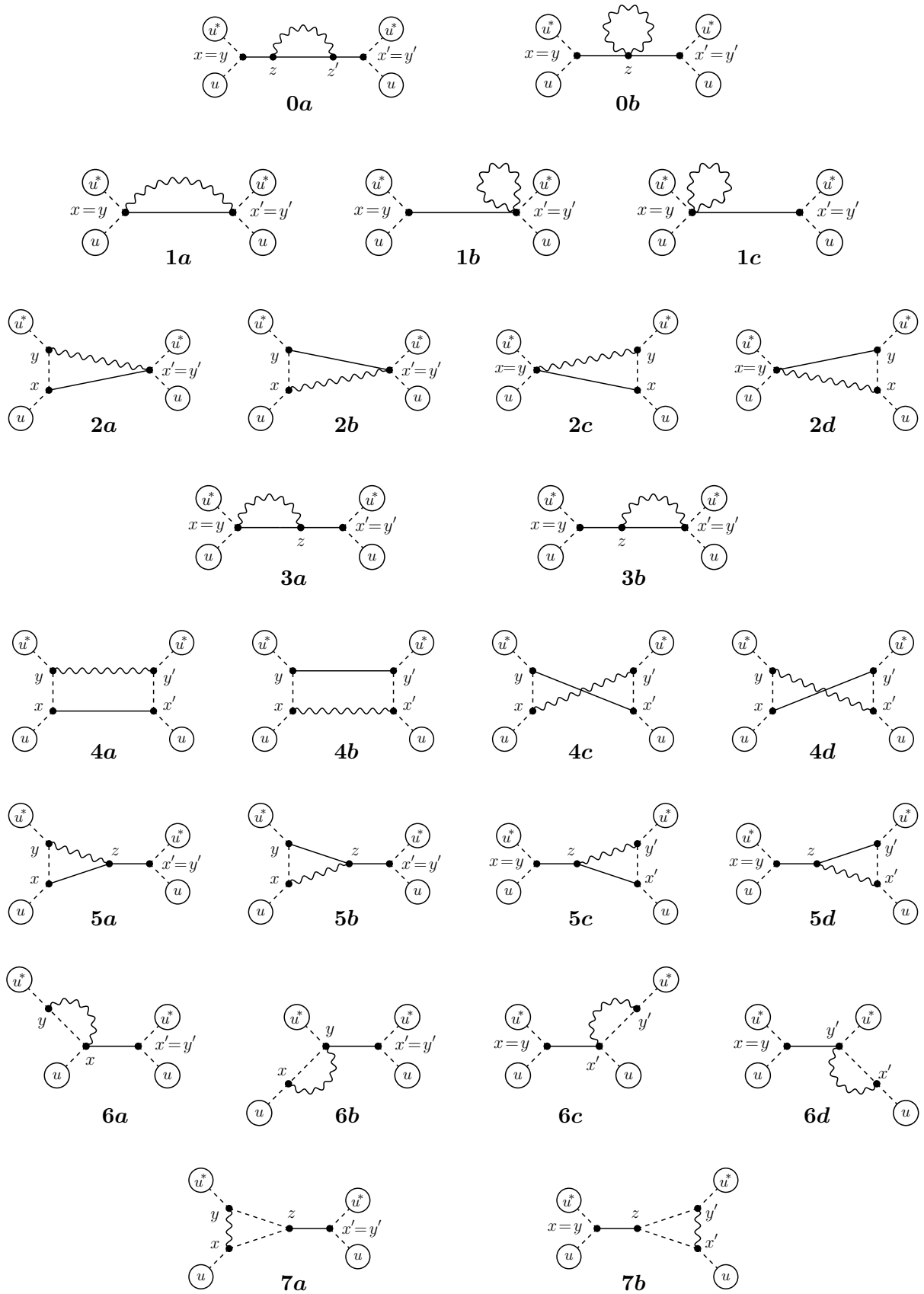


Figure 1: Eight classes of one-loop diagrams contributing to the t -channel of the connected four-point function, that is put on shell by the attached mode functions.

4.1 One-loop diagrams for 4-point functions

In what follows we list the eight classes of diagrams that we consider, which we denote by $0, 1, \dots, 7$, that are diagrammatically given in Fig. 1.

Class 0. The self-mass diagrams are comprised of two diagrams depicted in the first line of Fig. 1. These 3-vertex and 4-vertex diagrams, respectively, are given by the following expressions:

$$-iV_{0a} = (\kappa\lambda)^2 \delta^D(x-y) \delta^D(x'-y') (a_x a_{x'})^D \int d^D z d^D z' (a_z a_{z'})^{D-2} \left[\bar{\partial}_z^\mu \partial_z^\nu - \frac{1}{2} \eta^{\mu\nu} (\bar{\partial}_z \cdot \partial_z) \right] \\ \times \left[\bar{\partial}_{z'}^\rho \partial_{z'}^\sigma - \frac{1}{2} \eta^{\rho\sigma} (\bar{\partial}_{z'} \cdot \partial_{z'}) \right] i\Delta_A(x; z) \left(\begin{array}{c} i[\mu\nu\Delta_{\rho\sigma}](z; z') \\ i\Delta_A(z; z') \end{array} \right) i\Delta_A(z'; x'), \quad (4.3)$$

$$-iV_{0b} = i(\kappa\lambda)^2 \delta^D(x-y) \delta^D(x'-y') (a_x a_{x'})^D \int d^D z d^D z' a_z^{D-2} \theta^{\omega\lambda\mu\nu\rho\sigma} \\ \times \bar{\partial}_\omega^z \bar{\partial}_\lambda^{z'} i\Delta_A(x; z) \left(\begin{array}{c} i[\mu\nu\Delta_{\rho\sigma}](z; z) \\ \delta^D(z-z') \end{array} \right) i\Delta_A(z'; x'), \quad (4.4)$$

where the constant tensor structure in the second expression is

$$\theta^{\omega\lambda\mu\nu\rho\sigma} = \eta^{\omega(\mu} \eta^{\nu)(\rho} \eta^{\sigma)\lambda} - \frac{1}{4} \eta^{\omega(\mu} \eta^{\nu)\lambda} \eta^{\rho\sigma} - \frac{1}{4} \eta^{\omega(\rho} \eta^{\sigma)\lambda} \eta^{\mu\nu} - \frac{1}{4} \eta^{\omega\lambda} \eta^{\mu(\rho} \eta^{\sigma)\nu} + \frac{1}{8} \eta^{\omega\lambda} \eta^{\mu\nu} \eta^{\rho\sigma}. \quad (4.5)$$

The full computation would require to include the counterterm diagram as well, as was done in [49]. However, since the $\Delta\alpha$ variation will produce a gauge independent primitive result, we do not need to consider renormalization to prove gauge independence.

Class 1. This class of diagrams corresponds to the second line in Fig. 1. It contains the diagram representing correlation between vertices,

$$-iV_{1a} = -\frac{1}{4} (\kappa\lambda)^2 \delta^D(x-y) \delta^D(x'-y') (a_x a_{x'})^D \eta^{\mu\nu} \eta^{\rho\sigma} i[\mu\nu\Delta_{\rho\sigma}](x; x') i\Delta_A(x; x'), \quad (4.6)$$

as well as the local graviton corrections to 3-vertices,

$$-iV_{1b} = \frac{1}{4} (\kappa\lambda)^2 \delta^D(x-y) \delta^D(x'-y') (a_x a_{x'})^D \\ \times \left[\eta^{\mu(\rho} \eta^{\sigma)\nu} - \frac{1}{2} \eta^{\mu\nu} \eta^{\rho\sigma} \right] i[\mu\nu\Delta_{\rho\sigma}](x; x) i\Delta_A(x; x'), \quad (4.7)$$

$$-iV_{1c} = \frac{1}{4} (\kappa\lambda)^2 \delta^D(x-y) \delta^D(x'-y') (a_x a_{x'})^D \\ \times \left[\eta^{\mu(\rho} \eta^{\sigma)\nu} - \frac{1}{2} \eta^{\mu\nu} \eta^{\rho\sigma} \right] i\Delta_A(x; x') i[\mu\nu\Delta_{\rho\sigma}](x'; x'). \quad (4.8)$$

Class 2. This class of diagrams corresponds to vertex-source and vertex-observer correlations, that are depicted in the third row of Fig. 1. The expressions corresponding to these diagrams are:

$$-iV_{2a} = -\frac{i}{2} (\kappa\lambda)^2 \delta^D(x'-y') (a_x a_{x'})^D a_y^{D-2} \\ \times \left[\bar{\partial}_y^\mu \partial_y^\nu - \frac{1}{2} \eta^{\mu\nu} (\bar{\partial}_y \cdot \partial_y + a_y^2 m^2) \right] i\Delta_m(x; y) \left(\begin{array}{c} i[\mu\nu\Delta_{\rho\sigma}](y; x') \\ i\Delta_A(x; x') \end{array} \right), \quad (4.9)$$

$$-iV_{2b} = -\frac{i}{2} (\kappa\lambda)^2 \delta^D(x'-y') (a_y a_{x'})^D a_x^{D-2} \\ \times \left[\bar{\partial}_x^\mu \partial_x^\nu - \frac{1}{2} \eta^{\mu\nu} (\bar{\partial}_x \cdot \partial_x + a_x^2 m^2) \right] i\Delta_m(x; y) \left(\begin{array}{c} i\Delta_A(y; x') \\ i[\mu\nu\Delta_{\rho\sigma}](x; x') \end{array} \right), \quad (4.10)$$

$$-iV_{2c} = -\frac{i}{2} (\kappa\lambda)^2 \delta^D(x-y) (a_x a_{x'})^D a_{y'}^{D-2} \\ \times \left[\bar{\partial}_{y'}^\rho \partial_{y'}^\sigma - \frac{1}{2} \eta^{\rho\sigma} (\bar{\partial}_{y'} \cdot \partial_{y'} + a_{y'}^2 m^2) \right] \left(\begin{array}{c} i[\mu\nu\Delta_{\rho\sigma}](x; y') \\ i\Delta_A(x; x') \end{array} \right) i\Delta_m(x'; y'), \quad (4.11)$$

$$\begin{aligned}
-iV_{2d} = & -\frac{i}{2}(\kappa\lambda)^2\delta^D(x-y)(a_x a_{y'})^D a_{x'}^{D-2} \\
& \times \left[\bar{\partial}_{x'}^\rho \partial_{x'}^\sigma - \frac{1}{2}\eta^{\rho\sigma}(\bar{\partial}_{x'} \cdot \partial_{x'} + a_{x'}^2 m^2) \right] \left(\begin{array}{c} i\Delta_A(x; y') \\ i[\mu \Delta_{\rho\sigma}](x; x') \end{array} \right) i\Delta_m(x'; y'). \quad (4.12)
\end{aligned}$$

Class 3. The fourth row of Fig. 1 two diagrams comprising this class, that accounts for correlations between vertices and the force carrier,

$$\begin{aligned}
-iV_{3a} = & -\frac{i}{2}(\kappa\lambda)^2\delta^D(x'-y')(a_x a_{x'})^D \int d^D z a_z^{D-2} \\
& \times \left[\bar{\partial}_z^\rho \partial_z^\sigma - \frac{1}{2}\eta^{\rho\sigma} \bar{\partial}_z \cdot \partial_z \right] \left(\begin{array}{c} i[\mu \Delta_{\rho\sigma}](x; z) \\ i\Delta_A(x; z) \end{array} \right) i\Delta_A(z; x'), \quad (4.13)
\end{aligned}$$

$$\begin{aligned}
-iV_{3b} = & -\frac{i}{2}(\kappa\lambda)^2\delta^D(x-y)(a_x a_{x'})^D \int d^D z a_z^{D-2} \\
& \times \left[\bar{\partial}_z^\mu \partial_z^\nu - \frac{1}{2}\eta^{\mu\nu} \bar{\partial}_z \cdot \partial_z \right] i\Delta_A(x; z) \left(\begin{array}{c} i[\mu\nu \Delta^\rho_\rho](z; x') \\ i\Delta_A(z; x') \end{array} \right). \quad (4.14)
\end{aligned}$$

Class 4. The four diagrams comprising the class 4 of (fifth row of Fig. 1) represent source-observer correlations,

$$\begin{aligned}
-iV_{4a} = & (\kappa\lambda)^2(a_x a_{x'})^D(a_y a_{y'})^{D-2} \left[\bar{\partial}_y^\mu \partial_y^\nu - \frac{1}{2}\eta^{\mu\nu}(\bar{\partial}_y \cdot \partial_y + a_y^2 m^2) \right] \\
& \times \left[\bar{\partial}_{y'}^\rho \partial_{y'}^\sigma - \frac{1}{2}\eta^{\rho\sigma}(\bar{\partial}_{y'} \cdot \partial_{y'} + a_{y'}^2 m^2) \right] i\Delta_m(x; y) \left(\begin{array}{c} i[\mu\nu \Delta_{\rho\sigma}](y; y') \\ i\Delta_A(x; x') \end{array} \right) i\Delta_m(x'; y'), \quad (4.15)
\end{aligned}$$

$$\begin{aligned}
-iV_{4b} = & (\kappa\lambda)^2(a_y a_{y'})^D(a_x a_{x'})^{D-2} \left[\bar{\partial}_x^\mu \partial_x^\nu - \frac{1}{2}\eta^{\mu\nu}(\bar{\partial}_x \cdot \partial_x + a_x^2 m^2) \right] \\
& \times \left[\bar{\partial}_{x'}^\rho \partial_{x'}^\sigma - \frac{1}{2}\eta^{\rho\sigma}(\bar{\partial}_{x'} \cdot \partial_{x'} + a_{x'}^2 m^2) \right] i\Delta_m(x; y) \left(\begin{array}{c} i\Delta_A(y; y') \\ i[\mu\nu \Delta_{\rho\sigma}](x; x') \end{array} \right) i\Delta_m(x'; y'), \quad (4.16)
\end{aligned}$$

$$\begin{aligned}
-iV_{4c} = & (\kappa\lambda)^2(a_y a_{x'})^D(a_x a_{y'})^{D-2} \left[\bar{\partial}_x^\mu \partial_x^\nu - \frac{1}{2}\eta^{\mu\nu}(\bar{\partial}_x \cdot \partial_x + a_x^2 m^2) \right] \\
& \times \left[\bar{\partial}_{y'}^\rho \partial_{y'}^\sigma - \frac{1}{2}\eta^{\rho\sigma}(\bar{\partial}_{y'} \cdot \partial_{y'} + a_{y'}^2 m^2) \right] i\Delta_m(x; y) \left(\begin{array}{c} i\Delta_A(y; x') \\ i[\mu\nu \Delta_{\rho\sigma}](x; y') \end{array} \right) i\Delta_m(x'; y'), \quad (4.17)
\end{aligned}$$

$$\begin{aligned}
-iV_{4d} = & (\kappa\lambda)^2(a_x a_{y'})^D(a_y a_{x'})^{D-2} \left[\bar{\partial}_y^\mu \partial_y^\nu - \frac{1}{2}\eta^{\mu\nu}(\bar{\partial}_y \cdot \partial_y + a_y^2 m^2) \right] \\
& \times \left[\bar{\partial}_{x'}^\rho \partial_{x'}^\sigma - \frac{1}{2}\eta^{\rho\sigma}(\bar{\partial}_{x'} \cdot \partial_{x'} + a_{x'}^2 m^2) \right] i\Delta_m(x; y) \left(\begin{array}{c} i[\mu\nu \Delta_{\rho\sigma}](y; x') \\ i\Delta_A(x; y') \end{array} \right) i\Delta_m(x'; y'). \quad (4.18)
\end{aligned}$$

Class 5. Correlations of the force carrier with the source and the observer are captured by diagrams in this class. They are given in the sixth line of Fig. 1, with expressions corresponding to them being:

$$\begin{aligned}
-iV_{5a} = & (\kappa\lambda)^2\delta^D(x'-y')(a_x a_{x'})^D \int d^D z (a_y a_z)^{D-2} \left[\bar{\partial}_y^\mu \partial_y^\nu - \frac{1}{2}\eta^{\mu\nu}(\bar{\partial}_y \cdot \partial_y + a_y^2 m^2) \right] \\
& \times \left[\bar{\partial}_z^\rho \partial_z^\sigma - \frac{1}{2}\eta^{\rho\sigma} \bar{\partial}_z \cdot \partial_z \right] i\Delta_m(x; y) \left(\begin{array}{c} i[\mu\nu \Delta_{\rho\sigma}](y; z) \\ i\Delta_A(x; z) \end{array} \right) i\Delta_A(z; x'), \quad (4.19)
\end{aligned}$$

$$\begin{aligned}
-iV_{5b} = & (\kappa\lambda)^2\delta^D(x'-y')(a_y a_{x'})^D \int d^D z (a_x a_z)^{D-2} \left[\bar{\partial}_x^\mu \partial_x^\nu - \frac{1}{2}\eta^{\mu\nu}(\bar{\partial}_x \cdot \partial_x + a_x^2 m^2) \right] \\
& \times \left[\bar{\partial}_z^\rho \partial_z^\sigma - \frac{1}{2}\eta^{\rho\sigma} \bar{\partial}_z \cdot \partial_z \right] i\Delta_m(x; y) \left(\begin{array}{c} i\Delta_A(y; z) \\ i[\mu\nu \Delta_{\rho\sigma}](x; z) \end{array} \right) i\Delta_A(z; x'), \quad (4.20)
\end{aligned}$$

$$\begin{aligned}
-iV_{5c} = & (\kappa\lambda)^2\delta^D(x-y)(a_x a_{x'})^D \int d^D z (a_z a_{y'})^{D-2} \left[\bar{\partial}_z^\mu \partial_z^\nu - \frac{1}{2}\eta^{\mu\nu} \bar{\partial}_z \cdot \partial_z \right] \\
& \times \left[\bar{\partial}_{y'}^\rho \partial_{y'}^\sigma - \frac{1}{2}\eta^{\rho\sigma}(\bar{\partial}_{y'} \cdot \partial_{y'} + a_{y'}^2 m^2) \right] i\Delta_A(x; z) \left(\begin{array}{c} i[\mu\nu \Delta_{\rho\sigma}](z; y') \\ i\Delta_A(z; x') \end{array} \right) i\Delta_m(x'; y'), \quad (4.21)
\end{aligned}$$

$$\begin{aligned}
-iV_{5d} &= (\kappa\lambda)^2 (a_x a_{y'})^D \delta^D(x-y) \int d^D z (a_z a_{x'})^{D-2} \left[\bar{\partial}_z^\mu \partial_z^\nu - \frac{1}{2} \eta^{\mu\nu} \bar{\partial}_z \cdot \partial_z \right] \\
&\quad \times \left[\bar{\partial}_{x'}^\rho \partial_{x'}^\sigma - \frac{1}{2} \eta^{\rho\sigma} (\bar{\partial}_{x'} \cdot \partial_{x'} + a_{x'}^2 m^2) \right] i\Delta_A(x; z) \left(\begin{array}{c} i\Delta_A(z; y') \\ i[\mu\nu\Delta_{\rho\sigma}](z; x') \end{array} \right) i\Delta_m(x'; y'). \quad (4.22)
\end{aligned}$$

Class 6. This class of diagrams, depicted in the seventh row in Fig. 1, was not considered previously in [49]. However, it is necessary to include it to prove gauge independence. These diagrams represent vertex-observer and vertex-source self-correlations,

$$\begin{aligned}
-iV_{6a} &= -\frac{i}{2} (\kappa\lambda)^2 \delta^D(x'-y') (a_x a_{x'})^D a_y^{D-2} \\
&\quad \times \left[\bar{\partial}_y^{(\rho} \partial_y^{\sigma)} - \frac{1}{2} \eta^{\rho\sigma} (\bar{\partial}_y \cdot \partial_y + a_y^2 m^2) \right] \eta^{\mu\nu} \left(\begin{array}{c} i[\mu\nu\Delta_{\rho\sigma}](x; y) \\ i\Delta_m(x; y) \end{array} \right) i\Delta_A(x; x'), \quad (4.23)
\end{aligned}$$

$$\begin{aligned}
-iV_{6b} &= -\frac{i}{2} (\kappa\lambda)^2 \delta^D(x'-y') (a_y a_{x'})^D a_x^{D-2} \\
&\quad \times \left[\bar{\partial}_x^{(\mu} \partial_x^{\nu)} - \frac{1}{2} \eta^{\mu\nu} (\bar{\partial}_x \cdot \partial_x + a_x^2 m^2) \right] \eta^{\rho\sigma} \left(\begin{array}{c} i\Delta_m(x; y) \\ i[\mu\nu\Delta_{\rho\sigma}](x; y) \end{array} \right) i\Delta_A(y; x'), \quad (4.24)
\end{aligned}$$

$$\begin{aligned}
-iV_{6c} &= -\frac{i}{2} (\kappa\lambda)^2 \delta^D(x-y) (a_x a_{x'})^D a_{y'}^{D-2} \\
&\quad \times \left[\bar{\partial}_{y'}^{(\rho} \partial_{y'}^{\sigma)} - \frac{1}{2} \eta^{\rho\sigma} (\bar{\partial}_{y'} \cdot \partial_{y'} + a_{y'}^2 m^2) \right] \eta^{\mu\nu} i\Delta_A(x; x') \left(\begin{array}{c} i[\mu\nu\Delta_{\rho\sigma}](x'; y') \\ i\Delta_m(x'; y') \end{array} \right), \quad (4.25)
\end{aligned}$$

$$\begin{aligned}
-iV_{6d} &= -\frac{i}{2} (\kappa\lambda)^2 \delta^D(x-y) (a_x a_{y'})^D a_{x'}^{D-2} \\
&\quad \times \left[\bar{\partial}_{x'}^{(\mu} \partial_{x'}^{\nu)} - \frac{1}{2} \eta^{\mu\nu} (\bar{\partial}_{x'} \cdot \partial_{x'} + a_{x'}^2 m^2) \right] \eta^{\rho\sigma} i\Delta_A(x; y') \left(\begin{array}{c} i\Delta_m(x'; y') \\ i[\mu\nu\Delta_{\rho\sigma}](x'; y') \end{array} \right). \quad (4.26)
\end{aligned}$$

Class 7. The last class of 4-point diagrams, corresponding to the last line in Fig. 1, were also not considered previously in [49], but we now find it to be necessary. The two diagrams comprising it represent source-source and observer-observer self-correlations,

$$\begin{aligned}
-iV_{7a} &= (\kappa\lambda)^2 \delta^D(x'-y') (a_x a_y)^{D-2} \left[\bar{\partial}_x^{(\mu} \partial_x^{\nu)} - \frac{1}{2} \eta^{\mu\nu} (\bar{\partial}_x \cdot \partial_x + a_x^2 m^2) \right] \\
&\quad \times \left[\bar{\partial}_y^{(\rho} \partial_y^{\sigma)} - \frac{1}{2} \eta^{\rho\sigma} (\bar{\partial}_y \cdot \partial_y + a_y^2 m^2) \right] \int d^D z (a_z a_{x'})^D i[\mu\nu\Delta_{\rho\sigma}](x; y) \left(\begin{array}{c} i\Delta_m(y; z) \\ i\Delta_m(x; z) \end{array} \right) i\Delta_A(z; x'), \quad (4.27)
\end{aligned}$$

$$\begin{aligned}
-iV_{7b} &= (\kappa\lambda)^2 \delta^D(x-y) (a'_x a'_y)^{D-2} \left[\bar{\partial}_{x'}^{(\mu} \partial_{x'}^{\nu)} - \frac{1}{2} \eta^{\mu\nu} (\bar{\partial}_{x'} \cdot \partial_{x'} + a_{x'}^2 m^2) \right] \\
&\quad \times \left[\bar{\partial}_{y'}^{(\rho} \partial_{y'}^{\sigma)} - \frac{1}{2} \eta^{\rho\sigma} (\bar{\partial}_{y'} \cdot \partial_{y'} + a_{y'}^2 m^2) \right] \int d^D z (a_x a_z)^D i\Delta_A(x; z) \left(\begin{array}{c} i\Delta_m(z; y') \\ i\Delta_m(z; x') \end{array} \right) i[\mu\nu\Delta_{\rho\sigma}](x'; y'). \quad (4.28)
\end{aligned}$$

4.2 Consolidated one-loop diagrams for the 4-point function

A considerable simplification for the contributing diagrams in classes 1–5 was realized in [49]. This simplification applies regardless of the graviton gauge, and is attained by the consolidation of some classes of diagrams, that is effectively captured by eliminating vertex D and modifying vertex B,

$$\text{vertex B} \longrightarrow \text{vertex } \bar{\text{B}}, \quad \text{vertex D} \longrightarrow 0, \quad (4.29)$$

where the new consolidated vertex is given by:

$$\bar{\text{B}} \quad \begin{array}{c} \text{---} \text{---} \text{---} \\ \text{1} \quad \text{---} \quad \text{---} \\ \text{---} \text{---} \text{---} \\ \text{2} \quad \text{---} \quad \text{---} \\ \text{---} \text{---} \text{---} \\ \text{3} \end{array} \quad -i\kappa \left[-a_x^{D-2} \partial_1^{(\mu} \partial_2^{\nu)} + \frac{1}{4} \eta^{\mu\nu} \mathcal{D}_3 \right]. \quad (4.30)$$

This consolidation collapses (i) diagram classes 2 and 4, together with diagram 1a, into a consolidated diagram class $\bar{4}$, given in the first row of Fig. 2, and (ii) diagram classes 3 and 5 into a consolidated diagram class $\bar{5}$, given in the second row of Fig 2. The two remaining diagrams in class 1 are henceforth referred to as class $\bar{1}$.

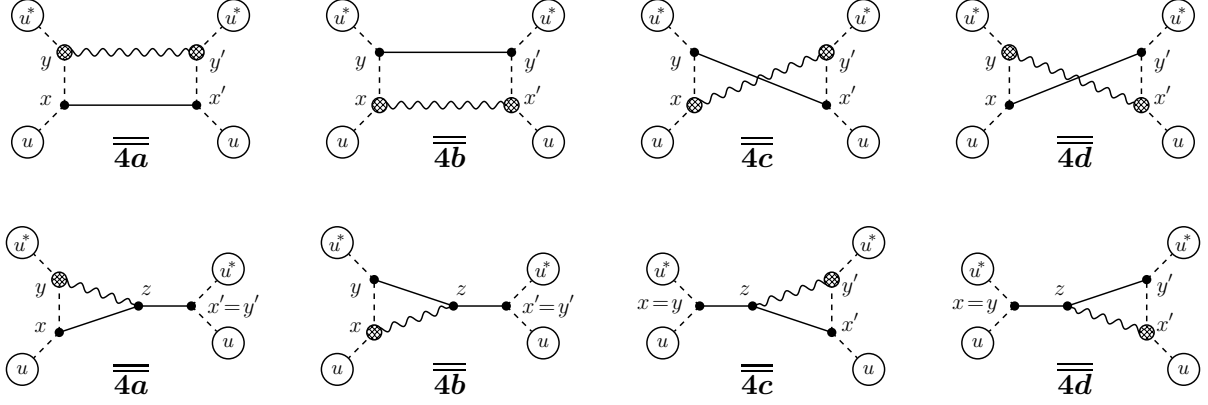


Figure 2: *First line:* diagram class $\bar{4}$ obtained by consolidating diagram classes in (4.15)–(4.18), and class 2 in (4.9)–(4.12), together with diagram 1a in (4.6). *Second line:* diagram class $\bar{5}$ obtained by consolidating diagrams from class 5 in (4.19)–(4.22), and class 3 in (4.13)–(4.14). The consolidated vertex \bar{B} , represented as a hatched vertex node, is defined in Eq. (4.30).

Class $\bar{4}$. The diagrams from classes 2 and 4, and the diagram 1a combine into four diagrams that make this new consolidated class:

$$\begin{aligned}
 -iV_{\bar{4a}} &= (\kappa\lambda)^2 (a_x a_{x'})^D \left[a_y^{D-2} \bar{\partial}_y^\mu \partial_y^\nu - \frac{1}{4} \eta^{\mu\nu} \tilde{\mathcal{D}}_y \right] \left[a_{y'}^{D-2} \bar{\partial}_{y'}^\rho \partial_{y'}^\sigma - \frac{1}{4} \eta^{\rho\sigma} \tilde{\mathcal{D}}_{y'} \right] \\
 &\quad \times i\Delta_m(x; y) \begin{pmatrix} i[\mu\nu\Delta_{\rho\sigma}](y; y') \\ i\Delta_A(x; x') \end{pmatrix} i\Delta_m(x'; y'), \quad (4.31)
 \end{aligned}$$

$$\begin{aligned}
 -iV_{\bar{4b}} &= (\kappa\lambda)^2 (a_y a_{y'})^D \left[a_x^{D-2} \bar{\partial}_x^\mu \partial_x^\nu - \frac{1}{4} \eta^{\mu\nu} \tilde{\mathcal{D}}_x \right] \left[a_{x'}^{D-2} \bar{\partial}_{x'}^\rho \partial_{x'}^\sigma - \frac{1}{4} \eta^{\rho\sigma} \tilde{\mathcal{D}}_{x'} \right] \\
 &\quad \times i\Delta_m(x; y) \begin{pmatrix} i\Delta_A(y; y') \\ i[\mu\nu\Delta_{\rho\sigma}](x; x') \end{pmatrix} i\Delta_m(x'; y'), \quad (4.32)
 \end{aligned}$$

$$\begin{aligned}
 -iV_{\bar{4c}} &= (\kappa\lambda)^2 (a_y a_{x'})^D \left[a_x^{D-2} \bar{\partial}_x^\mu \partial_x^\nu - \frac{1}{4} \eta^{\mu\nu} \tilde{\mathcal{D}}_x \right] \left[a_{y'}^{D-2} \bar{\partial}_{y'}^\rho \partial_{y'}^\sigma - \frac{1}{4} \eta^{\rho\sigma} \tilde{\mathcal{D}}_{y'} \right] \\
 &\quad \times i\Delta_m(x; y) \begin{pmatrix} i\Delta_A(y; x') \\ i[\mu\nu\Delta_{\rho\sigma}](x; y') \end{pmatrix} i\Delta_m(x'; y'), \quad (4.33)
 \end{aligned}$$

$$\begin{aligned}
 -iV_{\bar{4d}} &= (\kappa\lambda)^2 (a_x a_{y'})^D \left[a_y^{D-2} \bar{\partial}_y^\mu \partial_y^\nu - \frac{1}{4} \eta^{\mu\nu} \tilde{\mathcal{D}}_y \right] \left[a_{x'}^{D-2} \bar{\partial}_{x'}^\rho \partial_{x'}^\sigma - \frac{1}{4} \eta^{\rho\sigma} \tilde{\mathcal{D}}_{x'} \right] \\
 &\quad \times i\Delta_m(x; y) \begin{pmatrix} i[\mu\nu\Delta_{\rho\sigma}](y; x') \\ i\Delta_A(x; y') \end{pmatrix} i\Delta_m(x'; y'). \quad (4.34)
 \end{aligned}$$

Class $\bar{5}$. This consolidated class is made up of four diagrams resulting from combining diagrams of classes 3 and 5:

$$\begin{aligned}
 -iV_{\bar{5a}} &= (\kappa\lambda)^2 \delta^D(x' - y') (a_x a_{x'})^D \left[a_y^{D-2} \bar{\partial}_y^\mu \partial_y^\nu - \frac{1}{4} \eta^{\mu\nu} \tilde{\mathcal{D}}_y \right] \int d^D z a_z^{D-2} \\
 &\quad \times \left[\bar{\partial}_z^\rho \partial_z^\sigma - \frac{1}{2} \eta^{\rho\sigma} \bar{\partial}_z \cdot \partial_z \right] i\Delta_m(x; y) \begin{pmatrix} i[\mu\nu\Delta_{\rho\sigma}](y; z) \\ i\Delta_A(x; z) \end{pmatrix} i\Delta_A(z; x'), \quad (4.35)
 \end{aligned}$$

$$\begin{aligned}
 -iV_{\bar{5b}} &= (\kappa\lambda)^2 \delta^D(x' - y') (a_y a_{x'})^D \left[a_x^{D-2} \bar{\partial}_x^\mu \partial_x^\nu - \frac{1}{4} \eta^{\mu\nu} \tilde{\mathcal{D}}_x \right] \int d^D z a_z^{D-2} \\
 &\quad \times \left[\bar{\partial}_z^\rho \partial_z^\sigma - \frac{1}{2} \eta^{\rho\sigma} \bar{\partial}_z \cdot \partial_z \right] i\Delta_m(x; y) \begin{pmatrix} i\Delta_A(y; z) \\ i[\mu\nu\Delta_{\rho\sigma}](x; z) \end{pmatrix} i\Delta_A(z; x'), \quad (4.36)
 \end{aligned}$$

$$-iV_{\bar{5c}} = (\kappa\lambda)^2 \delta^D(x - y) (a_x a_{x'})^D \left[a_{y'}^{D-2} \bar{\partial}_{y'}^\mu \partial_{y'}^\nu - \frac{1}{4} \eta^{\mu\nu} \tilde{\mathcal{D}}_{y'} \right] \int d^D z a_z^{D-2}$$

$$\times \left[\bar{\partial}_z^\rho \partial_z^\sigma - \frac{1}{2} \eta^{\rho\sigma} \bar{\partial}_z \cdot \partial_z \right] i\Delta_A(x; z) \left(\begin{array}{c} i[\rho\sigma\Delta_{\mu\nu}](z; y') \\ i\Delta_A(z; x') \end{array} \right) i\Delta_m(x'; y'), \quad (4.37)$$

$$\begin{aligned} -iV_{\overline{5d}} &= (\kappa\lambda)^2 \delta^D(x-y) (a_x a_{y'})^D \left[a_{x'}^{D-2} \bar{\partial}_{x'}^\mu \partial_{x'}^\nu - \frac{1}{4} \eta^{\mu\nu} \tilde{\mathcal{D}}_{x'} \right] \int d^D z a_z^{D-2} \\ &\times \left[\bar{\partial}_z^\rho \partial_z^\sigma - \frac{1}{2} \eta^{\rho\sigma} \bar{\partial}_z \cdot \partial_z \right] i\Delta_A(x; z) \left(\begin{array}{c} i\Delta_A(z; y') \\ i[\rho\sigma\Delta_{\mu\nu}](z; x') \end{array} \right) i\Delta_m(x'; y'). \end{aligned} \quad (4.38)$$

4.3 One-loop diagrams for mode function corrections

The one-loop diagrams corresponding to the mode function corrections in the second line of (3.15) are given by, respectively,

$$(\text{Diag. } \delta u, a) = -\lambda^2 \int d^D x u(x) \delta u^*(x) \int d^D x' u(x') u^*(x') \times i\Delta_A(x; x'), \quad (4.39)$$

$$(\text{Diag. } \delta u, b) = -\lambda^2 \int d^D x \delta u(x) u^*(x) \int d^D x' u(x') u^*(x') \times i\Delta_A(x; x'), \quad (4.40)$$

$$(\text{Diag. } \delta u, c) = -\lambda^2 \int d^D x u(x) u^*(x) \int d^D x' u(x') \delta u^*(x') \times i\Delta_A(x; x'), \quad (4.41)$$

$$(\text{Diag. } \delta u, d) = -\lambda^2 \int d^D x u(x) u^*(x) \int d^D x' \delta u(x') u^*(x') \times i\Delta_A(x; x'), \quad (4.42)$$

with δu being the one-loop correction to the mode function coming from solving (3.16).

The mode function equation is corrected by the one-loop self-mass for the massive scalar. We split this self-mass into two parts, one made up of 3-vertices, and another made up of a 4-vertex, diagrammatically depicted in Fig. 3. The expressions corresponding to the two self-mass



Figure 3: One-loop diagrams representing contributions to the self-mass of the massive scalar field: the 3-vertex diagram (I) and the 4-vertex diagram (II).

contributions are given by

$$\begin{aligned} -i\mathcal{M}_I^2(x; y) &= -\kappa^2 (a_x a_y)^{D-2} \left[\bar{\partial}_x^{(\mu} \partial_x^{\nu)} - \frac{1}{2} \eta^{\mu\nu} (\bar{\partial}_x \cdot \partial_x + a_x^2 m^2) \right] \\ &\times \left[\bar{\partial}_y^{(\rho} \partial_y^{\sigma)} - \frac{1}{2} \eta^{\rho\sigma} (\bar{\partial}_y \cdot \partial_y + a_y^2 m^2) \right] \left(\begin{array}{c} i[\mu\nu\Delta_{\rho\sigma}](x; y) \\ i\Delta_m(x; y) \end{array} \right), \end{aligned} \quad (4.43)$$

$$\begin{aligned} -i\mathcal{M}_{II}^2(x; y) &= -i\kappa^2 \delta^D(x-y) a_x^{D-2} \left[\frac{1}{2} \bar{\partial}_x^{(\mu} \eta^{\nu)(\rho} \bar{\partial}_y^{\sigma)} + \frac{1}{2} \bar{\partial}_x^{(\rho} \eta^{\sigma)(\mu} \bar{\partial}_y^{\nu)} - \frac{1}{4} \bar{\partial}_x^{(\mu} \bar{\partial}_y^{\nu)} \eta^{\rho\sigma} - \frac{1}{4} \bar{\partial}_x^{(\rho} \bar{\partial}_y^{\sigma)} \eta^{\mu\nu} \right. \\ &\left. - \frac{1}{8} (2\eta^{\mu(\rho} \eta^{\sigma)\nu} - \eta^{\mu\nu} \eta^{\rho\sigma}) (\bar{\partial}_x \cdot \bar{\partial}_y + a_x^2 m^2) \right] i[\mu\nu\Delta_{\rho\sigma}](x; y), \end{aligned} \quad (4.44)$$

where we interpret barred derivatives as acting outside on whatever attaches to the self-mass, in line with the conventions in the rest of the paper. Accordingly, we split the corrections to mode functions into two classes as well, $\delta u = \delta u_I + \delta u_{II}$, each sourced by the corresponding contribution to the self-mass,

$$(\mathcal{D}_x - a_x^D m^2) \delta u_N(x) = \int d^D y \mathcal{M}_N^2(x; y) u(y), \quad N = I, II, \quad (4.45)$$

where in this equation all external x -derivatives in the self-mass are reflected to act on the self-mass.

5 Propagators

The diagrammatics of the preceding subsection are independent of the choice of gauge for the graviton propagator. Here we collect expressions and results for the scalar propagators and the graviton propagator in the simple one-parameter gauge, that we will use to evaluate the diagrams.

The propagator for a scalar field of mass M in de Sitter space satisfies the following equation of motion

$$(\mathcal{D}_x - a_x^D M^2) i\Delta_M(x; x') = i\delta^D(x - x'). \quad (5.1)$$

The solutions to this equation are de Sitter invariant for $M^2 > 0$ [83], but break de Sitter invariance already in the massless limit $M^2 = 0$ [84, 85], and also for tachyonic masses $M^2 < 0$ [86]. Apart from the scalar propagator with a heavy mass $m/H \gg 1$, whose specific form we will not need, we will need four scalar propagators with specific masses:

$$M_W^2 = -DH^2, \quad M_A^2 = 0, \quad M_B^2 = (D-2)H^2, \quad M_C^2 = 2(D-3)H^2. \quad (5.2)$$

The first two will thus contain de Sitter breaking parts, while the last two will be completely de Sitter invariant. Their power-series representations are [87]:

$$\begin{aligned} i\Delta_W(x; x') = & \frac{H^{D-2}}{(4\pi)^{\frac{D}{2}}} \left\{ \Gamma\left(\frac{D-2}{2}\right) \left(\frac{4}{y}\right)^{\frac{D-2}{2}} + \frac{4\Gamma\left(\frac{D+2}{2}\right)}{(D-4)(D-2)} \left(\frac{4}{y}\right)^{\frac{D-4}{2}} + \frac{2\Gamma\left(\frac{D+6}{2}\right)}{(D-6)(D-4)} \left(\frac{4}{y}\right)^{\frac{D-6}{2}} \right. \\ & + \frac{\Gamma(D)}{\Gamma\left(\frac{D}{2}\right)} \left[\frac{D+1}{2D} + (D-1)a_x a_{x'} - \frac{1}{D-1} \left(\frac{a_x}{a_{x'}} + \frac{a_{x'}}{a_x} \right) \right] \\ & + \frac{\Gamma(D)}{2\Gamma\left(\frac{D}{2}\right)} \left[\psi\left(-\frac{D}{2}\right) - \psi\left(\frac{D+1}{2}\right) - \psi(D+1) + \gamma_E - \frac{2\ln(a_x a_{x'})}{D+1} \right] (y-2) \\ & \left. + \sum_{n=2}^{\infty} \left[\frac{\Gamma\left(\frac{D+4}{2}+n\right)}{(n-\frac{D-4}{2})(n-\frac{D-2}{2})(n-1)!} \left(\frac{y}{4}\right)^{n-\frac{D-4}{2}} - \frac{\Gamma(n+D)}{n(n-1)\Gamma\left(n+\frac{D}{2}\right)} \left(\frac{y}{4}\right)^n \right] \right\}, \quad (5.3) \end{aligned}$$

$$\begin{aligned} i\Delta_A(x; x') = & \frac{H^{D-2}}{(4\pi)^{\frac{D}{2}}} \left\{ \Gamma\left(\frac{D-2}{2}\right) \left(\frac{4}{y}\right)^{\frac{D-2}{2}} + \frac{2\Gamma\left(\frac{D+2}{2}\right)}{D-4} \left(\frac{4}{y}\right)^{\frac{D-4}{2}} + \frac{\Gamma(D-1)}{\Gamma\left(\frac{D}{2}\right)} \left[\ln(aa') + \Psi \right] \right. \\ & \left. - \sum_{n=1}^{\infty} \left[\frac{\Gamma\left(\frac{D+2}{2}+n\right)}{\left(\frac{4-D}{2}+n\right)(n+1)!} \left(\frac{y}{4}\right)^{n-\frac{D-4}{2}} - \frac{\Gamma(D-1+n)}{n\Gamma\left(\frac{D}{2}+n\right)} \left(\frac{y}{4}\right)^n \right] \right\}, \quad (5.4) \end{aligned}$$

$$\begin{aligned} i\Delta_B(x; x') = & \frac{H^{D-2}}{(4\pi)^{\frac{D}{2}}} \left\{ \Gamma\left(\frac{D-2}{2}\right) \left(\frac{4}{y}\right)^{\frac{D-2}{2}} + \sum_{n=0}^{\infty} \left[\frac{\Gamma\left(\frac{D}{2}+n\right)}{(n+1)!} \left(\frac{y}{4}\right)^{n-\frac{D-4}{2}} - \frac{\Gamma(D-2+n)}{\Gamma\left(\frac{D}{2}+n\right)} \left(\frac{y}{4}\right)^n \right] \right\}, \quad (5.5) \end{aligned}$$

$$\begin{aligned} i\Delta_C(x; x') = & \frac{H^{D-2}}{(4\pi)^{\frac{D}{2}}} \left\{ \Gamma\left(\frac{D-2}{2}\right) \left(\frac{4}{y}\right)^{\frac{D-2}{2}} - \sum_{n=0}^{\infty} \left[\frac{\left(\frac{6-D}{2}+n\right)\Gamma\left(\frac{D-2}{2}+n\right)}{(n+1)!} \left(\frac{y}{4}\right)^{n-\frac{D-4}{2}} \right. \right. \\ & \left. \left. - \frac{\Gamma(D-3+n)(1+n)}{\Gamma\left(\frac{D}{2}+n\right)} \left(\frac{y}{4}\right)^n \right] \right\}, \quad (5.6) \end{aligned}$$

where $\Psi = -\psi\left(\frac{2-D}{2}\right) + \psi\left(\frac{D-1}{2}\right) + \psi(D-1) - \gamma_E$.

We will need a particular kind of integrated propagator that satisfies equations sourced by scalar propagators,

$$(\mathcal{D}_x - a_x^D M_I^2) K_{IJ}(x; x') = a_x^{D-2} i\Delta_J(x; x'), \quad (\mathcal{D}_{x'} - a_{x'}^D M_J^2) K_{IJ}(x; x') = a_{x'}^{D-2} i\Delta_I(x; x'), \quad (5.7)$$

so that its solution can be written in an integral form [47],

$$K_{IJ}(x; x') = -i \int d^D z a_z^{D-2} i\Delta_I(x; z) i\Delta_J(z; x'). \quad (5.8)$$

In particular we will need its two diagonal instances, that can be evaluated in terms of differences of ordinary scalar propagators [48],

$$K_{AA}(x; x') = \frac{i\Delta_B(x; x') - i\Delta_W(x; x')}{2(D-1)H^2 a_x a_{x'}}, \quad K_{BB}(x; x') = \frac{i\Delta_C(x; x') - i\Delta_A(x; x')}{2(D-3)H^2 a_x a_{x'}}. \quad (5.9)$$

Using the results for the scalar propagators collected above we can write the graviton propagator in the simple one-parameter gauge [47, 48],

$$i[\mu\nu\Delta_{\rho\sigma}](x; x') = i[\mu\nu\Delta_{\rho\sigma}](x; x')\Big|_{\alpha=1} + \Delta\alpha \times i[\mu\nu\Theta_{\rho\sigma}](x; x'), \quad (5.10)$$

where $\Delta\alpha = \alpha - 1$ can take arbitrary finite values. The first term is the graviton propagator in the simplest gauge [21, 22],

$$\begin{aligned} i[\mu\nu\Delta_{\rho\sigma}](x; x')\Big|_{\alpha=1} &= 2\left[\bar{\eta}_{\rho(\mu}\bar{\eta}_{\nu)\sigma} - \frac{\bar{\eta}_{\mu\nu}\bar{\eta}_{\rho\sigma}}{D-3}\right]i\Delta_A(x; x') - 4\delta_{(\mu}^0\bar{\eta}_{\nu)(\rho}\delta_{\sigma)}^0 i\Delta_B(x; x') \\ &+ \frac{2}{(D-2)(D-3)}\left[\bar{\eta}_{\mu\nu} + (D-3)\delta_{\mu}^0\delta_{\nu}^0\right]\left[\bar{\eta}_{\rho\sigma} + (D-3)\delta_{\rho}^0\delta_{\sigma}^0\right]i\Delta_C(x; x'), \end{aligned} \quad (5.11)$$

corresponding to the choice $\alpha = 1$ for the gauge-fixing parameter. The computation in that gauge has been reported in [49]. Here we are interested in computing the $\Delta\alpha$ contribution in the one-parameter simple gauge, and proving gauge independence. This requires us to recompute all the diagrams using the second part of the graviton propagator in (5.10),

$$i[\mu\nu\Theta_{\rho\sigma}](x; x') = -4\partial_{(\mu}^x\bar{\eta}_{\nu)(\rho}\partial_{\sigma)}^{x'}K_{AA}(x; x') + 4\left[\delta_{(\mu}^0\partial_{\nu)}^x - \eta_{\mu\nu}Ha_x\right]\left[\delta_{(\rho}^0\partial_{\sigma)}^{x'} - \eta_{\rho\sigma}Ha_{x'}\right]K_{BB}(x; x'). \quad (5.12)$$

that we call the $\Delta\alpha$ variation.

Note that the derivative operators acting on integrated propagators in the graviton propagator annihilate some of the terms in the power-series expansion of specific propagators (5.3)–(5.6), so that we can drop them from the integrated propagators. In this paper we will need only the dimensionally regulated coincidence limits of the AA integrated propagator and its first two derivatives,

$$K_{AA}(x; x') \xrightarrow{x' \rightarrow x} \frac{-k}{H^2 a_x^2} \left[\ln(a_x) + \frac{\Psi}{2} + \frac{2D-3}{2(D-2)} \right], \quad (5.13)$$

$$\partial_{\mu}^x K_{AA}(x; x') \xrightarrow{x' \rightarrow x} \frac{k\delta_{\mu}^0}{H a_x} \left[\ln(a_x) + \frac{\Psi-1}{2} + \frac{2D-3}{2(D-2)} \right], \quad (5.14)$$

$$\partial_{\mu}^x \partial_{\nu}^{x'} K_{AA}(x; x') \xrightarrow{x' \rightarrow x} -k \left[\left(\ln(a_x) + \frac{\Psi+1}{2} \right) \bar{\eta}_{\mu\nu} - \frac{(D-3)}{2(D-2)} \delta_{\mu}^0 \delta_{\nu}^0 \right], \quad (5.15)$$

and the same for the BB integrated propagator,

$$K_{BB}(x; x') \xrightarrow{x' \rightarrow x} \frac{-k}{(D-3)H^2 a_x^2} \left[\ln(a_x) + \frac{\Psi}{2} - \frac{1}{2(D-2)(D-3)} \right], \quad (5.16)$$

$$\partial_{\mu}^x K_{BB}(x; x') \xrightarrow{x' \rightarrow x} \frac{k\delta_{\mu}^0}{(D-3)H a_x} \left[\ln(a_x) + \frac{\Psi-1}{2} - \frac{1}{2(D-2)(D-3)} \right], \quad (5.17)$$

$$\partial_{\mu}^x \partial_{\nu}^{x'} K_{BB}(x; x') \xrightarrow{x' \rightarrow x} \frac{-k}{(D-3)} \left[\left(\ln(a_x) + \frac{\Psi-3}{2} + \frac{D-4}{2(D-2)(D-3)} \right) \delta_{\mu}^0 \delta_{\nu}^0 + \frac{D-3}{2(D-2)} \bar{\eta}_{\mu\nu} \right]. \quad (5.18)$$

where we introduced a dimensionful constant

$$k = \frac{H^{D-2}}{(4\pi)^{\frac{D}{2}}} \frac{\Gamma(D-1)}{\Gamma(\frac{D}{2})}. \quad (5.19)$$

These limits are obtained from (5.3)–(5.6) and (5.9). We will only be using the logarithm parts of these coincidence limits, as only they are connected to the large logarithmic correction of the exchange potential that we are interested in. However, since the logarithm always comes together with the divergent constant Ψ in the same combination, our proof of the cancellation of gauge dependence for the $\Delta\alpha$ part also holds true for one-loop divergences.

6 Reducing 4-point diagrams

It is convenient to break up the computation of the 4-point diagrams in Fig. 1 into two parts, one coming from the $\Delta\alpha$ variation of the graviton propagator (5.12) containing K_{AA} , and the other part containing K_{BB} ; accordingly we refer to these parts as AA and BB .

6.1 Preliminary reduction of AA parts

In each of the diagrams from classes 0–7 we need to contract the tensor structure of the two vertices (either \bar{B} , C, or B) into the tensor structure of the AA part of the graviton propagator. There are three different contractions of a single vertex into the AA tensor structure. Contracting the C-vertex gives

$$a_z^{D-2} \left[\bar{\partial}_z^\mu \partial_z^\nu - \frac{1}{2} \eta^{\mu\nu} \bar{\partial}_z \cdot \partial_z \right] \times \left[-4 \tilde{\partial}_{(\mu}^z \bar{\eta}_{\nu)(\rho} \tilde{\partial}_{\sigma)}^{z'} \right] = -2a_z^{D-2} \left[(\bar{\partial}_z \cdot \tilde{\partial}_z) \nabla_{(\rho}^z \tilde{\partial}_{\sigma)}^{z'} \right. \\ \left. + (\partial_z \cdot \tilde{\partial}_z) \bar{\nabla}_{(\rho}^z \tilde{\partial}_{\sigma)}^{z'} - (\bar{\partial}_z \cdot \partial_z) \tilde{\nabla}_{(\rho}^z \tilde{\partial}_{\sigma)}^{z'} \right] \longrightarrow 2D_z \bar{\nabla}_{(\rho}^z \tilde{\partial}_{\sigma)}^{z'} + 2\bar{D}_z \nabla_{(\rho}^z \tilde{\partial}_{\sigma)}^{z'}. \quad (6.1)$$

Here the first equality is obtained by just expanding out the product and contracting the indices. Getting to the final expression required the use of the second vertex identity (3.5) for contracted derivatives, followed by the first vertex identity (3.4) applied to spatial derivatives. Applying the same sequence of operations we derive the contraction of the \bar{B} -vertex into the graviton AA tensor structure,

$$\left[a_z^{D-2} \bar{\partial}_z^\mu \partial_z^\nu - \frac{1}{4} \eta^{\mu\nu} \tilde{\mathcal{D}}_z \right] \times \left[-4 \tilde{\partial}_{(\mu}^z \bar{\eta}_{\nu)(\rho} \tilde{\partial}_{\sigma)}^{z'} \right] = -2a_z^{D-2} (\bar{\partial}_z \cdot \tilde{\partial}_z) \nabla_{(\rho}^z \tilde{\partial}_{\sigma)}^{z'} \\ - 2a_z^{D-2} (\partial_z \cdot \tilde{\partial}_z) \bar{\nabla}_{(\rho}^z \tilde{\partial}_{\sigma)}^{z'} + \tilde{D}_z \tilde{\nabla}_{(\rho}^z \tilde{\partial}_{\sigma)}^{z'} \longrightarrow (D_z - \bar{D}_z) (2\bar{\nabla}_{(\rho}^z + \tilde{\nabla}_{(\rho}^z) \tilde{\partial}_{\sigma)}^{z'}). \quad (6.2)$$

and also the contraction of the B-vertex,

$$a_z^{D-2} \left[\bar{\partial}_z^{(\mu} \partial_z^{\nu)} - \frac{1}{2} \eta^{\mu\nu} (\bar{\partial}_z \cdot \partial_z + a_z^2 m^2) \right] \times \left[-4 \tilde{\partial}_{(\mu}^z \bar{\eta}_{\nu)(\rho} \tilde{\partial}_{\sigma)}^{z'} \right] \\ = -2a_z^{D-2} \left[(\bar{\partial}_z \cdot \tilde{\partial}_z) \nabla_{(\rho}^z \tilde{\partial}_{\sigma)}^{z'} + (\partial_z \cdot \tilde{\partial}_z) \bar{\nabla}_{(\rho}^z \tilde{\partial}_{\sigma)}^{z'} - (\bar{\partial}_z \cdot \partial_z + a_z^2 m^2) \tilde{\nabla}_{(\rho}^z \tilde{\partial}_{\sigma)}^{z'} \right] \\ \longrightarrow 2(D_z - a_z^D m^2) \bar{\nabla}_{(\rho}^z \tilde{\partial}_{\sigma)}^{z'} + 2(\bar{D}_z - a_z^D m^2) \nabla_{(\rho}^z \tilde{\partial}_{\sigma)}^{z'}. \quad (6.3)$$

We give contractions of the second vertex as needed for each diagram class.

Diagram class 0. There are two C-vertices in the $0a$ diagram (4.3), which requires contracting the second C-vertex into (6.1) to obtain the necessary contraction,

$$a_z^{D-2} \left[\bar{\partial}_z^\mu \partial_z^\nu - \frac{1}{2} \eta^{\mu\nu} \bar{\partial}_z \cdot \partial_z \right] \times \left[-4 \tilde{\partial}_{(\mu}^z \bar{\eta}_{\nu)(\rho} \tilde{\partial}_{\sigma)}^{z'} \right] \times a_{z'}^{D-2} \left[\bar{\partial}_{z'}^\rho \partial_{z'}^\sigma - \frac{1}{2} \eta^{\rho\sigma} \bar{\partial}_{z'} \cdot \partial_{z'} \right] \\ = a_{z'}^{D-2} \left[\bar{D}_z (\nabla_z \cdot \bar{\nabla}_{z'}) (\tilde{\partial}_{z'} \cdot \partial_{z'}) + \bar{D}_z (\nabla_z \cdot \nabla_{z'}) (\tilde{\partial}_{z'} \cdot \bar{\partial}_{z'}) - \bar{D}_z (\nabla_z \cdot \tilde{\nabla}_{z'}) (\bar{\partial}_{z'} \cdot \partial_{z'}) \right. \\ \left. + D_z (\bar{\nabla}_z \cdot \bar{\nabla}_{z'}) (\tilde{\partial}_{z'} \cdot \partial_{z'}) + D_z (\bar{\nabla}_z \cdot \nabla_{z'}) (\tilde{\partial}_{z'} \cdot \bar{\partial}_{z'}) - D_z (\bar{\nabla}_z \cdot \tilde{\nabla}_{z'}) (\bar{\partial}_{z'} \cdot \partial_{z'}) \right] \\ \longrightarrow -\bar{D}_z (\nabla_z \cdot \nabla_{z'}) \bar{D}_{z'} - \bar{D}_z (\nabla_z \cdot \bar{\nabla}_{z'}) D_{z'} - D_z (\bar{\nabla}_z \cdot \nabla_{z'}) \bar{D}_{z'} - D_z (\bar{\nabla}_z \cdot \bar{\nabla}_{z'}) D_{z'}. \quad (6.4)$$

Just as for the first set of contractions, we first expanded out the product, and then used the second vertex identity, followed by the first vertex identity applied to spatial derivatives to obtain

the final result. Substituting this contraction into diagram (4.3), using the equation of motion for the A -type scalar propagator (5.1), and unpacking the condensed notation produces

$$\begin{aligned} \left[-iV_{0a}\right]_{AA}^{\Delta\alpha} &= (\kappa\lambda)^2\delta^D(x-y)\delta^D(x'-y')(a_x a_{x'})^D \left\{ K_{AA}(x; x') \times \nabla_x \cdot \nabla_{x'} i\Delta_A(x; x') \right. \\ &\quad + \nabla_y \cdot \left[K_{AA}(x; y) \times \nabla_y i\Delta_A(y; x') \right] + \nabla_{y'} \cdot \left[\nabla_{y'} i\Delta_A(x; y') \times K_{AA}(y'; x') \right] \\ &\quad \left. - i \int d^D z d^D z' \left[\nabla_z^\mu i\Delta_A(x; z) \right] \left(\frac{K_{AA}(z; z')}{\mathcal{D}_z \delta^D(z-z')} \right) \left[\nabla_\mu^{z'} i\Delta_A(z'; x') \right] \right\}. \end{aligned} \quad (6.5)$$

Diagram 0b in (4.4) requires the contraction of the constant tensor structure (4.5) and the two derivatives in (4.4) into the AA graviton tensor structure. Upon performing that contraction, and after using the fact that in the coincident limit, $z' \rightarrow z$, spatial derivatives acting on the graviton propagator can be reflected as $\tilde{\nabla}_z \leftrightarrow -\tilde{\nabla}_{z'}$, we obtain

$$\begin{aligned} \left[-iV_{0b}\right]_{AA}^{\Delta\alpha} &= i(\kappa\lambda)^2\delta^D(x-y)\delta^D(x'-y')(a_x a_{x'})^D \int d^D z a_z^{D-2} \partial_\mu^z i\Delta_A(x; z) \\ &\quad \times \left\{ \left[\frac{1}{2}(D-1)\eta^{\mu\nu}\partial_z \cdot \partial_{z'} - (D-1)\partial_z^\mu \partial_{z'}^\nu - \bar{\eta}^{\mu\nu}\partial_z \cdot \partial_{z'} \right] K_{AA}(z; z') \right\}_{z' \rightarrow z} \times \partial_\nu^z i\Delta_A(z; x'), \end{aligned} \quad (6.6)$$

where the condensed notation has been unpacked.

Diagram class $\bar{1}$. Diagrams 1b and 1c in (4.7) and (4.8) require the contraction of the simple constant tensor structure in the G -vertex into the tensor structure of the AA part of the graviton propagator,

$$\left[\eta^{\mu(\rho}\eta^{\sigma)\nu} - \frac{1}{2}\eta^{\mu\nu}\eta^{\rho\sigma} \right] \times \left[-4\tilde{\partial}_{(\mu}^z \bar{\eta}_{\nu)(\rho} \tilde{\partial}_{\sigma)}^{z'} \right] = -2(D-1)(\tilde{\partial}_z \cdot \tilde{\partial}_{z'}). \quad (6.7)$$

Applying this to the two diagrams then yields

$$\left[-iV_{1b}\right]_{AA}^{\Delta\alpha} = -\frac{1}{2}(D-1)(\kappa\lambda)^2\delta^D(x-y)\delta^D(x'-y')(a_x a_{x'})^D \left[\partial_x \cdot \partial_y K_{AA}(x; y) \right] \times i\Delta_A(x; x'), \quad (6.8)$$

$$\left[-iV_{1c}\right]_{AA}^{\Delta\alpha} = -\frac{1}{2}(D-1)(\kappa\lambda)^2\delta^D(x-y)\delta^D(x'-y')(a_x a_{x'})^D i\Delta_A(x; x') \times \left[\partial_{x'} \cdot \partial_{y'} K_{AA}(x'; y') \right]. \quad (6.9)$$

Diagram class $\bar{4}$. The tensor contractions necessary for the $\bar{4}$ diagrams are obtained by contracting another \bar{B} -vertex into (6.2).

$$\begin{aligned} &\left[a_z^{D-2} \bar{\partial}_z^\mu \partial_z^\nu - \frac{1}{4}\eta^{\mu\nu} \bar{\mathcal{D}}_z \right] \times \left[-4\tilde{\partial}_{(\mu}^z \bar{\eta}_{\nu)(\rho} \tilde{\partial}_{\sigma)}^{z'} \right] \times \left[a_{z'}^{D-2} \bar{\partial}_{z'}^\rho \partial_{z'}^\sigma - \frac{1}{4}\eta^{\rho\sigma} \bar{\mathcal{D}}_{z'} \right] \\ &= \frac{1}{2}a_{z'}^{D-2} (\mathcal{D}_z - \bar{\mathcal{D}}_z) (2\bar{\nabla}_z + \tilde{\nabla}_z) \cdot \left[\bar{\nabla}_{z'} (\tilde{\partial}_{z'} \cdot \partial_{z'}) + \nabla_{z'} (\tilde{\partial}_{z'} \cdot \bar{\partial}_{z'}) - \frac{1}{2}\tilde{\nabla}_{z'} \bar{\mathcal{D}}_{z'} \right] \\ &\longrightarrow -\frac{1}{4}(\mathcal{D}_z - \bar{\mathcal{D}}_z) (2\bar{\nabla}_z + \tilde{\nabla}_z) \cdot (2\bar{\nabla}_{z'} + \tilde{\nabla}_{z'}) (\mathcal{D}_{z'} - \bar{\mathcal{D}}_{z'}). \end{aligned} \quad (6.10)$$

We arrive at this result by applying the second vertex identity (3.5), followed by the first vertex identity (3.4) applied to the spatial derivatives. Substituting this contraction into the diagram $\bar{4a}$ in (4.31) we have

$$\begin{aligned} \left[-iV_{\bar{4a}}\right]_{AA}^{\Delta\alpha} &= -\frac{(\kappa\lambda)^2}{4} (a_x a_{x'})^D (2\bar{\nabla}_y + \tilde{\nabla}_y) \cdot (2\bar{\nabla}_{y'} + \tilde{\nabla}_{y'}) \\ &\quad \times (\mathcal{D}_y - \bar{\mathcal{D}}_y) i\Delta_m(x; y) \left(\frac{K_{AA}(y; y')}{i\Delta_A(x; x')} \right) (\mathcal{D}_{y'} - \bar{\mathcal{D}}_{y'}) i\Delta_m(x'; y'). \end{aligned} \quad (6.11)$$

There are two favorable combinations of derivatives, each of which pinches one massive propagator, owing to $\overline{\mathcal{D}}$ producing $a^D m^2$ when acting on the external mode function according to (3.14),

$$(\mathcal{D}_y - \overline{\mathcal{D}}_y) i\Delta_m(x; y) \longrightarrow (\mathcal{D}_y - a_y^D m^2) i\Delta_m(x; y) = i\delta^D(x - y). \quad (6.12)$$

This reduces the diagram to the topology of the first diagram on the right-hand side of (3.3) by eliminating massive propagators from it,

$$\left[-iV_{\overline{4a}}\right]_{AA}^{\Delta\alpha} = \frac{(\kappa\lambda)^2}{4} (a_x a_{x'})^D \delta^D(x - y) \delta^D(x' - y') (2\overline{\nabla}_y + \tilde{\nabla}_y) \cdot (2\overline{\nabla}_{y'} + \tilde{\nabla}_{y'}) \begin{pmatrix} K_{AA}(y; y') \\ i\Delta_A(x; x') \end{pmatrix}. \quad (6.13)$$

However, this form is still not amenable to be interpreted as the effective self-mass contribution on account of the derivatives acting on external mode functions. These derivatives can be moved away from external mode functions, and into the loop only after the $\overline{4a}$ contribution is combined with the tree remaining ones $\overline{4b}$, $\overline{4c}$, and $\overline{4d}$, that are obtained by reflecting the coordinates,

$$\left[-iV_{\overline{4b}}\right]_{AA}^{\Delta\alpha} = \frac{(\kappa\lambda)^2}{4} \delta^D(x - y) \delta^D(x' - y') (a_y a_{y'})^D (2\overline{\nabla}_x + \tilde{\nabla}_x) \cdot (2\overline{\nabla}_{x'} + \tilde{\nabla}_{x'}) \begin{pmatrix} i\Delta_A(y; y') \\ K_{AA}(x; x') \end{pmatrix}, \quad (6.14)$$

$$\left[-iV_{\overline{4c}}\right]_{AA}^{\Delta\alpha} = \frac{(\kappa\lambda)^2}{4} \delta^D(x - y) (a_y a_{x'})^D \delta^D(x' - y') (2\overline{\nabla}_x + \tilde{\nabla}_x) \cdot (2\overline{\nabla}_{y'} + \tilde{\nabla}_{y'}) \begin{pmatrix} i\Delta_A(y; x') \\ K_{AA}(x; y') \end{pmatrix}, \quad (6.15)$$

$$\left[-iV_{\overline{4d}}\right]_{AA}^{\Delta\alpha} = \frac{(\kappa\lambda)^2}{4} \delta^D(x - y) \delta^D(x' - y') (a_x a_{y'})^D (2\overline{\nabla}_y + \tilde{\nabla}_y) \cdot (2\overline{\nabla}_{x'} + \tilde{\nabla}_{x'}) \begin{pmatrix} K_{AA}(y; x') \\ i\Delta_A(x; y') \end{pmatrix}. \quad (6.16)$$

Adding these contributions together, and making use of the delta functions in vertices produces a relatively simple expression,

$$\left[-iV_{\overline{4a+b+c+d}}\right]_{AA}^{\Delta\alpha} = (\kappa\lambda)^2 \delta^D(x - y) \delta^D(x' - y') (a_x a_{x'})^D \times (\overline{\nabla}_y + \overline{\nabla}_x + \tilde{\nabla}_y) \cdot (\overline{\nabla}_{y'} + \overline{\nabla}_{x'} + \tilde{\nabla}_{y'}) \begin{pmatrix} K_{AA}(y; y') \\ i\Delta_A(x; x') \end{pmatrix}. \quad (6.17)$$

Upon closer examination, we may use the first vertex identity (3.4) to move spatial derivatives onto the scalar propagator, thus obtaining the final expression that, after unpacking the notation, reads

$$\left[-iV_{\overline{4a+b+c+d}}\right]_{AA}^{\Delta\alpha} = (\kappa\lambda)^2 \delta^D(x - y) \delta^D(x' - y') (a_x a_{x'})^D \times K_{AA}(x; x') \left[\nabla_x \cdot \nabla_{x'} i\Delta_A(x; x') \right]. \quad (6.18)$$

Diagram class $\overline{5}$. For this class of diagrams we need to contract the $\overline{\mathbf{B}}$ -vertex into (6.2), which is done following the same sequence of operations as for the other contractions in this section,

$$\begin{aligned} & \left[a_z^{D-2} \overline{\partial}_z^\mu \partial_z^\nu - \frac{1}{4} \eta^{\mu\nu} \overline{\mathcal{D}}_z \right] \times \left[-4 \tilde{\partial}_{(\mu}^z \overline{\eta}_{\nu)(\rho} \tilde{\partial}_{\sigma)}^z \right] \times a_{z'}^{D-2} \left[\overline{\partial}_{z'}^\rho \partial_{z'}^\sigma - \frac{1}{2} \eta^{\rho\sigma} \overline{\partial}_{z'} \cdot \partial_{z'} \right] \\ & = \frac{1}{2} a_{z'}^{D-2} (\mathcal{D}_z - \overline{\mathcal{D}}_z) (2\overline{\nabla}_z + \tilde{\nabla}_z) \cdot \left[\overline{\nabla}_{z'} (\tilde{\partial}_{z'} \cdot \partial_{z'}) + \nabla_{z'} (\tilde{\partial}_{z'} \cdot \partial_{z'}) - \tilde{\nabla}_{z'} (\overline{\partial}_{z'} \cdot \partial_{z'}) \right] \\ & \longrightarrow -\frac{1}{2} (\mathcal{D}_z - \overline{\mathcal{D}}_z) (2\overline{\nabla}_z + \tilde{\nabla}_z) \cdot \left(\nabla_{z'} \overline{\mathcal{D}}_{z'} + \overline{\nabla}_{z'} \mathcal{D}_{z'} \right). \end{aligned} \quad (6.19)$$

Applying this contraction to diagram $\overline{5a}$ in (4.19) gives

$$\begin{aligned} \left[-iV_{\overline{5a}}\right]_{AA}^{\Delta\alpha} &= -\frac{(\kappa\lambda)^2}{2} \delta^D(x' - y') (a_x a_{x'})^D \int d^D z' (\mathcal{D}_y - \overline{\mathcal{D}}_y) i\Delta_m(x; y) \\ &\times (2\overline{\nabla}_y + \tilde{\nabla}_y) \cdot \left[\begin{pmatrix} K_{AA}(y; z') \\ \nabla_{z'} i\Delta_A(x; z') \end{pmatrix} \overline{\mathcal{D}}_{z'} i\Delta_A(z'; x') + \begin{pmatrix} K_{AA}(y; z') \\ \mathcal{D}_{z'} i\Delta_A(x; z') \end{pmatrix} \overline{\nabla}_{z'} i\Delta_A(z'; x') \right], \end{aligned} \quad (6.20)$$

where accents on derivatives still denote where they act, but where we have in addition distributed the derivatives to make the following steps more obvious. Pinching the massive propagator by the favorable combination of derivatives, and also an additional A -type scalar propagator in each term then gives

$$\begin{aligned} \left[-iV_{\overline{5a}}\right]_{AA}^{\Delta\alpha} &= \frac{(\kappa\lambda)^2}{2}\delta^D(x-y)\delta^D(x'-y')(a_x a_{x'})^D \\ &\quad \times (2\overline{\nabla}_y + \widetilde{\nabla}_y) \cdot \left[K_{AA}(y; x') \nabla_{x'} i\Delta_A(x; x') + K_{AA}(y; x) \nabla_x i\Delta_A(x; x') \right]. \end{aligned} \quad (6.21)$$

Here the barred derivative acts on the corresponding external leg, while the tilded derivative acts on the AA integrated propagator descended from the graviton propagator.

The $\overline{5b}$ diagram is obtained by interchanging the coordinate arguments $x \leftrightarrow y$. However, due to the delta function identifying the points x and y the two diagrams only differ in the derivative acting on the external leg, and combine together into

$$\begin{aligned} \left[-iV_{\overline{5a+b}}\right]_{AA}^{\Delta\alpha} &= (\kappa\lambda)^2\delta^D(x-y)\delta^D(x'-y')(a_x a_{x'})^D \\ &\quad \times (\overline{\nabla}_x + \overline{\nabla}_y + \widetilde{\nabla}_x) \cdot \left[K_{AA}(x; x') \nabla_{x'} i\Delta_A(y; x') + K_{AA}(x; y) \nabla_y i\Delta_A(y; x') \right]. \end{aligned} \quad (6.22)$$

We can now apply the first vertex identity (3.4) for the spatial derivatives in the $x=y$ vertex; for the first term in the brackets this is effectively a 5-point vertex, while for the second term this is effectively a 4-point vertex,

$$\begin{aligned} \left[-iV_{\overline{5a+b}}\right]_{AA}^{\Delta\alpha} &= -(\kappa\lambda)^2\delta^D(x-y)\delta^D(x'-y')(a_x a_{x'})^D \\ &\quad \times \left\{ K_{AA}(x; x') \nabla_x \cdot \nabla_{x'} i\Delta_A(x; x') + \nabla_y \cdot \left[K_{AA}(x; y) \times \nabla_y i\Delta_A(y; x') \right] \right\}. \end{aligned} \quad (6.23)$$

The remaining two diagrams $\overline{5c}$ and $\overline{5d}$ are obtained from this result by simultaneously exchanging coordinate arguments $(x, y) \leftrightarrow (x', y')$,

$$\begin{aligned} \left[-iV_{\overline{5c+d}}\right]_{AA}^{\Delta\alpha} &= -(\kappa\lambda)^2\delta^D(x-y)\delta^D(x'-y')(a_x a_{x'})^D \\ &\quad \times \left\{ K_{AA}(x; x') \nabla_x \cdot \nabla_{x'} i\Delta_A(x; x') + \nabla_{y'} \cdot \left[\nabla_{y'} i\Delta_A(x; y') \times K_{AA}(y'; x') \right] \right\}. \end{aligned} \quad (6.24)$$

Diagram class 6. For the four diagrams in this class we need to take the trace of the contraction (6.3),

$$\begin{aligned} a_z^{D-2} \left[\overline{\partial}_z^{(\mu} \partial_z^{\nu)} - \frac{1}{2} \eta^{\mu\nu} (\overline{\partial}_z \cdot \partial_z + a_z^2 m^2) \right] &\times \left[-4 \widetilde{\partial}_{(\mu}^z \overline{\eta}_{\nu)(\rho} \widetilde{\partial}_{\sigma)}^z \right] \eta^{\rho\sigma} \\ &\longrightarrow 2(\mathcal{D}_z - a_z^D m^2) (\overline{\nabla}_z \cdot \widetilde{\nabla}_{z'}) + 2(\overline{\mathcal{D}}_z - a_z^D m^2) (\nabla_z \cdot \widetilde{\nabla}_{z'}). \end{aligned} \quad (6.25)$$

Substituting this into the diagram (4.23) gives

$$\left[-iV_{6a}\right]_{AA}^{\Delta\alpha} = \frac{1}{2}(\kappa\lambda)^2\delta^D(x-y)\delta^D(x'-y')(a_x a_{x'})^D \overline{\nabla}_x \cdot \nabla_x K_{AA}(x; x) \times i\Delta_A(x; x'), \quad (6.26)$$

where we used that

$$\delta^D(x-y) \partial_\mu^x K_{AA}(x; y) = \frac{1}{2} \delta^D(x-y) \partial_\mu^x K_{AA}(x; x). \quad (6.27)$$

After adding to (6.26) the $6b$ diagram, obtained by reflecting $x \leftrightarrow y$, we can get rid of derivatives acting on external mode functions by integrating by parts,

$$\left[-iV_{6a+b}\right]_{AA}^{\Delta\alpha} = -\frac{1}{2}(\kappa\lambda)^2\delta^D(x-y)\delta^D(x'-y')(a_x a_{x'})^D \nabla_x \cdot \left[\nabla_x K_{AA}(x; x) \times i\Delta_A(x; x') \right]. \quad (6.28)$$

The sum of the two remaining diagrams is then obtained by reflecting pairs of coordinates $(x, y) \leftrightarrow (x', y')$ in the expression above,

$$\left[-iV_{6c+d}\right]_{AA}^{\Delta\alpha} = -\frac{1}{2}(\kappa\lambda)^2\delta^D(x-y)\delta^D(x'-y')(a_x a_{x'})^D \nabla_{x'} \cdot \left[i\Delta_A(x; x') \times \nabla_{x'} K_{AA}(x'; x') \right]. \quad (6.29)$$

Diagram class 7. The last diagram class from Fig. 1 requires contracting another B-vertex into (6.3),

$$\begin{aligned}
& a_z^{D-2} \left[\bar{\partial}_z^{(\mu} \partial_z^{\nu)} - \frac{1}{2} \eta^{\mu\nu} (\bar{\partial}_z \cdot \partial_z + a_z^2 m^2) \right] \times \left[-4 \tilde{\partial}_{(\mu}^z \bar{\eta}_{\nu)(\rho} \tilde{\partial}_{\sigma)}^z \right] \times a_{z'}^{D-2} \left[\bar{\partial}_{z'}^{(\rho} \partial_{z'}^{\sigma)} - \frac{1}{2} \eta^{\rho\sigma} (\bar{\partial}_{z'} \cdot \partial_{z'} + a_{z'}^2 m^2) \right] \\
&= a_{z'}^{D-2} (\mathcal{D}_z - a_z^D m^2) \left[(\bar{\nabla}_z \cdot \bar{\nabla}_{z'}) (\tilde{\partial}_{z'} \cdot \partial_{z'}) + (\bar{\nabla}_z \cdot \nabla_{z'}) (\tilde{\partial}_{z'} \cdot \bar{\partial}_{z'}) - (\bar{\nabla}_z \cdot \tilde{\nabla}_{z'}) (\bar{\partial}_{z'} \cdot \partial_{z'} + a_{z'}^D m^2) \right] \\
&\quad + a_{z'}^{D-2} (\bar{\mathcal{D}}_z - a_z^D m^2) \left[(\nabla_z \cdot \bar{\nabla}_{z'}) (\tilde{\partial}_{z'} \cdot \partial_{z'}) + (\nabla_z \cdot \nabla_{z'}) (\tilde{\partial}_{z'} \cdot \bar{\partial}_{z'}) - (\bar{\nabla}_z \cdot \tilde{\nabla}_{z'}) (\bar{\partial}_{z'} \cdot \partial_{z'} + a_{z'}^D m^2) \right] \\
&\rightarrow - (\mathcal{D}_z - a_z^D m^2) (\bar{\nabla}_z \cdot \bar{\nabla}_{z'}) (\mathcal{D}_{z'} - a_{z'}^D m^2) - (\mathcal{D}_z - a_z^D m^2) (\bar{\nabla}_z \cdot \nabla_{z'}) (\bar{\mathcal{D}}_{z'} - a_{z'}^D m^2) \\
&\quad - (\bar{\mathcal{D}}_z - a_z^D m^2) (\nabla_z \cdot \bar{\nabla}_{z'}) (\mathcal{D}_{z'} - a_{z'}^D m^2) - (\bar{\mathcal{D}}_z - a_z^D m^2) (\nabla_z \cdot \nabla_{z'}) (\bar{\mathcal{D}}_{z'} - a_{z'}^D m^2). \tag{6.30}
\end{aligned}$$

This result is reached by first expanding the expression and contracting all the indices. This is followed by applying the second vertex identity (3.5) to contracted spacetime derivatives, and then the first vertex identity (3.4) to spatial derivatives. Using this contraction for the diagram 7a in (4.27), and using equations of motion for the external mode functions and the massive propagator, we get

$$\left[-iV_{7a} \right]_{AA}^{\Delta\alpha} = (\kappa\lambda)^2 \delta^D(x-y) \delta^D(x'-y') (a_x a_{x'})^D \bar{\nabla}_x \cdot \bar{\nabla}_y \times K_{AA}(x; x) i\Delta_A(x; x'). \tag{6.31}$$

Even though this result is reduced to the topology of the third diagram on the right-hand side of (3.3), it is not in the form that can be interpreted directly as contributing to the effective self-mass. This is because the two contracted derivatives still act on external mode functions. The same is true for the other diagram of this class that is obtained by reflecting pairs of coordinates,

$$\left[-iV_{7b} \right]_{AA}^{\Delta\alpha} = (\kappa\lambda)^2 \delta^D(x-y) \delta^D(x'-y') (a_x a_{x'})^D i\Delta_A(x; x') K_{AA}(x'; x') \times \bar{\nabla}_{x'} \cdot \bar{\nabla}_{y'}. \tag{6.32}$$

Nevertheless, this will not be an obstacle in the end, as this contribution will be canceled by a contribution coming from the external mode function corrections.

Cancellation of non-local contributions. Diagram 0a, and diagrams from classes $\bar{4}$ and $\bar{5}$ contain non-local contributions, while all the other diagrams contain contributions of the same topology as the first diagram on the right-hand side of (3.3). These contributions can rightfully be called non-local, compared to the contributions from the other diagrams, that take the form of local vertex corrections. It is therefore natural to consider them together. In fact, when taken together their non-local contributions all cancel,

$$\begin{aligned}
& \left[-iV_{0a} - iV_{\overline{4a+b+c+d}} - iV_{\overline{5a+b+c+d}} \right]_{AA}^{\Delta\alpha} = -(\kappa\lambda)^2 \delta^D(x-y) \delta^D(x'-y') (a_x a_{x'})^D \\
& \quad \times i \int d^D z d^D z' \left[\nabla_z^\mu i\Delta_A(x; z) \right] \left(\frac{K_{AA}(z; z')}{\mathcal{D}_z \delta^D(z-z')} \right) \left[\nabla_\mu^{z'} i\Delta_A(z'; x') \right]. \tag{6.33}
\end{aligned}$$

The remaining contribution can be further reduced, but we first need to migrate derivatives away from the delta function. We do this by first symmetrizing the derivatives acting on the delta function,

$$\mathcal{D}_z \delta^D(z-z') = -\partial_z \cdot \partial_{z'} [a_z^{D-2} \delta^D(z-z')], \tag{6.34}$$

and then integrating by parts each derivative around its vertex. This frees up the delta function so that we can integrate over it,

$$\begin{aligned}
& \left[-iV_{0a} - iV_{\overline{4a+b+c+d}} - iV_{\overline{5a+b+c+d}} \right]_{AA}^{\Delta\alpha} = (\kappa\lambda)^2 \delta^D(x-y) \delta^D(x'-y') (a_x a_{x'})^D \\
& \quad \times i \int d^D z a_z^{D-2} \left\{ \frac{1}{2} \partial_z^\nu \nabla_z^\mu i\Delta_A(x; z) \times \partial_\nu^z [K_{AA}(z; z) \times \nabla_\mu^{z'} i\Delta_A(z; x')] \right\}
\end{aligned}$$

$$\begin{aligned}
& + \frac{1}{2} \partial_z^\nu \left[\nabla_z^\mu i \Delta_A(x; z) \times K_{AA}(z; z) \right] \times \partial_\nu^z \nabla_\mu^z i \Delta_A(z; x') \\
& + \left[\nabla_z^\mu i \Delta_A(x; z) \right] \times \left[\partial_z \cdot \partial_{z'} K_{AA}(z; z') \right]_{z \rightarrow z'} \times \left[\nabla_\mu^z i \Delta_A(z; x') \right] \Big\}, \quad (6.35)
\end{aligned}$$

where we have used (6.27). Now integrating by parts the derivative in the first two terms in braces of (6.35) produces the scalar d'Alembertian \mathcal{D} that eliminates a single scalar leg in each term. This finally produces,

$$\begin{aligned}
& \left[-iV_{0a} - iV_{\frac{4a+b+c+d}{4a+b+c+d}} - iV_{\frac{5a+b+c+d}{5a+b+c+d}} \right]_{AA}^{\Delta\alpha} = (\kappa\lambda)^2 \delta^D(x-y) \delta^D(x'-y') (a_x a_{x'})^D \\
& \times \left\{ -\frac{1}{2} \nabla_x \cdot \left[K_{AA}(x; x) \times \nabla_x i \Delta_A(x; x') \right] - \frac{1}{2} \nabla_{x'} \cdot \left[\nabla_{x'} i \Delta_A(x; x') \times K_{AA}(x'; x') \right] \right. \\
& \left. + i \int d^D z a_z^{D-2} \left[\nabla_z^\mu i \Delta_A(x; z) \right] \times \left[\partial_z \cdot \partial_{z'} K_{AA}(z; z') \right]_{z' \rightarrow z} \times \left[\nabla_\mu^z i \Delta_A(z; x') \right] \right\}. \quad (6.36)
\end{aligned}$$

6.2 Preliminary reduction of BB parts

The tensor structure of the BB part of the graviton propagator factorizes, and consequently so do the contractions needed for the diagrams of Fig. 1. There are three contractions we need, the first one with the C-vertex,

$$\begin{aligned}
& a_z^{D-2} \left[\bar{\partial}_z^\mu \partial_z^\nu - \frac{1}{2} \eta^{\mu\nu} \bar{\partial}_z \cdot \partial_z \right] \times 2 \left[\delta_{(\mu}^0 \tilde{\partial}_{\nu)}^z - \eta_{\mu\nu} H a_z \right] \\
& = a_z^{D-2} \left[-(\partial_z \cdot \tilde{\partial}_z) \bar{\partial}_0^z - (\bar{\partial}_z \cdot \tilde{\partial}_z) \partial_0^z + (\bar{\partial}_z \cdot \partial_z) \left(\tilde{\partial}_0^z + (D-2) H a_z \right) \right] \\
& \longrightarrow a_z^{D-2} \left[-\partial_z \cdot (\tilde{\partial}_z + \bar{\partial}_z) \bar{\partial}_0^z - \bar{\partial}_z \cdot (\tilde{\partial}_z + \partial_z) \partial_0^z \right] \longrightarrow \mathcal{D}_z \bar{\partial}_0^z + \bar{\mathcal{D}}_z \partial_0^z. \quad (6.37)
\end{aligned}$$

Here we first expanded the expression and contracted indices, followed by partially integrating the uncontracted derivative in the last term using the first vertex identity (3.4), to then apply the second vertex identity (3.5) to the contracted derivatives. The second contraction we need is with the \bar{B} -vertex,

$$\begin{aligned}
& \left[a_z^{D-2} \bar{\partial}_z^\mu \partial_z^\nu - \frac{1}{4} \eta^{\mu\nu} \bar{\mathcal{D}}_z \right] \times 2 \left[\delta_{(\mu}^0 \tilde{\partial}_{\nu)}^z - \eta_{\mu\nu} H a_z \right] \\
& = -a_z^{D-2} \left[(\partial_z \cdot \tilde{\partial}_z) \bar{\partial}_0^z + (\bar{\partial}_z \cdot \tilde{\partial}_z) \partial_0^z + 2H a_z (\bar{\partial}_z \cdot \partial_z) \right] + \frac{1}{2} \bar{\mathcal{D}}_z (\tilde{\partial}_0^z + D H a_z) \\
& \longrightarrow \frac{1}{2} (\mathcal{D}_z - \bar{\mathcal{D}}_z) (\bar{\partial}_0^z - \partial_0^z) + H a_z (\mathcal{D}_z + \bar{\mathcal{D}}_z) + \frac{1}{2} \bar{\mathcal{D}}_z \left[\tilde{\partial}_0^z + \bar{\partial}_0^z + \partial_0^z + (D-2) H a_z \right] \\
& \longrightarrow \frac{1}{2} \left[\bar{\partial}_0^z - \partial_0^z + D H a_z \right] (\mathcal{D}_z - \bar{\mathcal{D}}_z) + D H a_z \bar{\mathcal{D}}_z + \frac{1}{2} (\tilde{\partial}_0^z + \bar{\partial}_0^z + \partial_0^z) \bar{\mathcal{D}}_z \\
& \longrightarrow \frac{1}{2} \left[2\bar{\partial}_0^z + \tilde{\partial}_0^z + D H a_z \right] (\mathcal{D}_z - \bar{\mathcal{D}}_z) + D H a_z \bar{\mathcal{D}}_z. \quad (6.38)
\end{aligned}$$

Deriving the final expression first required explicitly contracting derivatives, and then applying the second vertex identity (3.5) to the contracted derivatives. Getting to the penultimate line required the use of commutation identities (3.7), followed by integrating derivatives by parts using the first vector identity (3.4) to get to the last expression. Lastly, we need the contraction with the B-vertex, that is obtained by the same sequence of steps,

$$\begin{aligned}
& a_z^{D-2} \left[\bar{\partial}_z^{(\mu} \partial_z^{\nu)} - \frac{1}{2} \eta^{\mu\nu} (\bar{\partial}_z \cdot \partial_z + a_z^2 m^2) \right] \times 2 \left[\delta_{(\mu}^0 \tilde{\partial}_{\nu)}^z - \eta_{\mu\nu} H a_z \right] \\
& = a_z^{D-2} \left[(\bar{\partial}_z \cdot \partial_z) (\tilde{\partial}_0^z + (D-2) H a_z) - (\partial_z \cdot \tilde{\partial}_z) \bar{\partial}_0^z - (\bar{\partial}_z \cdot \tilde{\partial}_z) \partial_0^z + a_z^2 m^2 (\tilde{\partial}_0^z + D H a_z) \right] \\
& \longrightarrow \frac{1}{2} \bar{\mathcal{D}}_z (\tilde{\partial}_0^z + \bar{\partial}_0^z + \partial_0^z) - \frac{1}{2} \bar{\mathcal{D}}_z (\tilde{\partial}_0^z + \bar{\partial}_0^z - \partial_0^z) - \frac{1}{2} \mathcal{D}_z (\tilde{\partial}_0^z - \bar{\partial}_0^z + \partial_0^z) \\
& \quad + \frac{1}{2} (D-2) H a_z (\bar{\mathcal{D}}_z - \bar{\mathcal{D}}_z - \mathcal{D}_z) - (D-2) H^2 a_z^D \bar{\partial}_0^z - m^2 a_z^D (\tilde{\partial}_0^z + D H a_z) \\
& \longrightarrow (\mathcal{D}_z - a_z^D m^2) \bar{\partial}_0^z + (\bar{\mathcal{D}}_z - a_z^D m^2) \partial_0^z. \quad (6.39)
\end{aligned}$$

Diagram class 0. The diagram in (4.3) requires two contractions in (6.37), one for each vertex. The operators in these contractions pinch the A -type propagators they act on, reducing the diagram to

$$\begin{aligned} \left[-iV_{0a}\right]_{BB}^{\Delta\alpha} &= (\kappa\lambda)^2\delta^D(x-y)\delta^D(x'-y')(a_x a_{x'})^D \left\{ -K_{BB}(x; x') \times \partial_0^x \partial_0^{x'} i\Delta_A(x; x') \right. \\ &\quad - \partial_0^y \left[K_{BB}(x; y) \times \partial_0^y i\Delta_A(y; x') \right] - \partial_0^{y'} \left[\partial_0^{y'} i\Delta_A(x; y') \times K_{BB}(y'; x') \right] \\ &\quad \left. + i \int d^D z d^D z' \left[\partial_0^z i\Delta_A(x; z) \right] \left(\frac{K_{BB}(z; z')}{\mathcal{D}_z \delta^D(z-z')} \right) \left[\partial_0^{z'} i\Delta_A(z'; x') \right] \right\}. \end{aligned} \quad (6.40)$$

For the $0b$ diagram in (4.4) we perform all the contractions, and use that any odd number of spatial derivatives acting on the graviton taken at coincidence vanishes,

$$\begin{aligned} \left[-iV_{0b}\right]_{BB}^{\Delta\alpha} &= (\kappa\lambda)^2\delta^D(x-y)\delta^D(x'-y')(a_x a_{x'})^D \times i \int d^D z a_z^{D-2} \\ &\quad \times \left[\partial_\mu^z i\Delta_A(x; z) \right] \times \left\{ \left[\frac{1}{2} \eta^{\mu\nu} (\partial_z \cdot \partial_{z'} + 2(D-4)H a_z \partial_0^z + (D-2)(D-4)H^2 a_z^2) \right. \right. \\ &\quad \left. \left. + \delta_0^\mu \delta_0^\nu (\partial_z \cdot \partial_{z'} + 2(D-4)H a_z \partial_0^z) - \partial_z^\mu \partial_{z'}^\nu \right] K_{BB}(z; z') \right\}_{z' \rightarrow z} \times \left[\partial_\nu^z i\Delta_A(z; x') \right]. \end{aligned} \quad (6.41)$$

Diagram class $\bar{1}$. For the two diagrams in this class we need the simple contraction

$$\begin{aligned} \left[\eta^{\mu(\rho} \eta^{\sigma)\nu} - \frac{1}{2} \eta^{\mu\nu} \eta^{\rho\sigma} \right] \times 4 \left[\delta_{(\mu}^0 \tilde{\partial}_{\nu)}^z - \eta_{\mu\nu} H a_z \right] \left[\delta_{(\rho}^0 \tilde{\partial}_{\sigma)}^{z'} - \eta_{\rho\sigma} H a_{z'} \right] \\ = -2(\tilde{\partial}_z \cdot \tilde{\partial}_{z'}) - 2(D-2) \left[H a_z \tilde{\partial}_0^{z'} + H a_{z'} \tilde{\partial}_0^z + D H^2 a_z a_{z'} \right]. \end{aligned} \quad (6.42)$$

Applied to diagrams in (4.7) and (4.8) this produces

$$\begin{aligned} \left[-iV_{1b}\right]_{BB}^{\Delta\alpha} &= -\frac{1}{2}(\kappa\lambda)^2\delta^D(x-y)\delta^D(x'-y')(a_x a_{x'})^D \\ &\quad \times \left\{ \left[\partial_x \cdot \partial_y + (D-2)(H a_x \partial_0^y + H a_y \partial_0^x + D H^2 a_x a_y) \right] K_{BB}(x; y) \right\} \times i\Delta_A(x; x'), \end{aligned} \quad (6.43)$$

$$\begin{aligned} \left[-iV_{1c}\right]_{BB}^{\Delta\alpha} &= -\frac{1}{2}(\kappa\lambda)^2\delta^D(x-y)\delta^D(x'-y')(a_x a_{x'})^D \\ &\quad \times i\Delta_A(x; x') \times \left\{ \left[\partial_{x'} \cdot \partial_{y'} + (D-2)(H a_{x'} \partial_0^{y'} + H a_{y'} \partial_0^{x'} + D H^2 a_{x'} a_{y'}) \right] K_{BB}(x'; y') \right\}. \end{aligned} \quad (6.44)$$

Diagram class $\bar{4}$. The $\bar{4a}$ diagram in (4.31) takes two contractions in (6.38),

$$\begin{aligned} \left[-iV_{\bar{4a}}\right]_{BB}^{\Delta\alpha} &= -\frac{1}{4}(\kappa\lambda)^2\delta^D(x-y)\delta^D(x'-y')(a_x a_{x'})^D \\ &\quad \times \left(2\bar{\partial}_0^y + \tilde{\partial}_0^y + D H a_y \right) \left(2\bar{\partial}_0^{y'} + \tilde{\partial}_0^{y'} + D H a_{y'} \right) \left(\frac{K_{BB}(y; y')}{i\Delta_A(x; x')} \right), \end{aligned} \quad (6.45)$$

By combining this with the remaining three diagrams (4.32)–(4.34) the derivatives in vertices combine neatly, and can be integrated by parts away from the external mode functions,

$$\left[-iV_{\frac{4a+b+c+d}{4}}\right]_{BB}^{\Delta\alpha} = -(\kappa\lambda)^2\delta^D(x-y)\delta^D(x'-y')(a_x a_{x'})^D K_{BB}(x; x') \times \partial_0^x \partial_0^{x'} i\Delta_A(x; x'). \quad (6.46)$$

Diagram class $\bar{5}$. Diagram $\bar{5a}$ from (4.35) requires the contraction in (6.38) for the y -vertex and contraction (6.37) for the z -vertex,

$$\left[-iV_{\bar{5a}}\right]_{BB}^{\Delta\alpha} = -\frac{1}{2}(\kappa\lambda)^2\delta^D(x-y)\delta^D(x'-y')(a_x a_{x'})^D$$

$$\times \left(2\bar{\partial}_0^y + \tilde{\partial}_0^y + DH a_y \right) \left[\left(\frac{K_{BB}(y; x')}{\partial_0^{x'} i \Delta_A(x; x')} \right) + \left(\frac{K_{BB}(y; x)}{\partial_0^x i \Delta_A(x; x')} \right) \right]. \quad (6.47)$$

Adding to it the $\bar{5b}$ contribution, obtained by reflecting coordinates, the derivatives in the second line combine into a vertex identity, and are integrated by parts to obtain

$$\begin{aligned} \left[-iV_{\bar{5a+b}} \right]_{BB}^{\Delta\alpha} &= (\kappa\lambda)^2 \delta^D(x-y) \delta^D(x'-y') (a_x a_{x'})^D \\ &\times \left\{ K_{BB}(x; x') \times \partial_0^x \partial_0^{x'} i \Delta_A(x; x') + \partial_0^y \left[K_{BB}(x; y) \times \partial_0^y i \Delta_A(y; x') \right] \right\}. \end{aligned} \quad (6.48)$$

The two remaining contributions $\bar{5c}$ and $\bar{5d}$ are obtained by interchanging pairs of coordinates,

$$\begin{aligned} \left[-iV_{\bar{5c+d}} \right]_{BB}^{\Delta\alpha} &= (\kappa\lambda)^2 \delta^D(x-y) \delta^D(x'-y') (a_x a_{x'})^D \\ &\times \left\{ K_{BB}(x; x') \times \partial_0^x \partial_0^{x'} i \Delta_A(x; x') + \partial_0^{y'} \left[K_{BB}(x'; y') \times \partial_0^{y'} i \Delta_A(x; y') \right] \right\}. \end{aligned} \quad (6.49)$$

Diagram class 6. For this class of diagrams, given in (4.23)–(4.26), we need the contraction in (6.39), and also to take the trace of one of the tensor structures in the BB part of graviton propagator,

$$\begin{aligned} \left[-iV_{6a} \right]_{BB}^{\Delta\alpha} &= i(\kappa\lambda)^2 \delta^D(x'-y') (a_x a_{x'})^D \\ &\times \left[(\mathcal{D}_y - a_y^D m^2) \bar{\partial}_0^y + (\bar{\mathcal{D}}_y - a_y^D m^2) \partial_0^y \right] (\tilde{\partial}_0^x + DH a_x) \left(\frac{K_{BB}(x; y)}{i \Delta_m(x; y)} \right) i \Delta_A(x; x'). \end{aligned} \quad (6.50)$$

Applying equations of motion we have

$$\left[-iV_{6a} \right]_{BB}^{\Delta\alpha} = -\frac{1}{2} (\kappa\lambda)^2 \delta^D(x-y) \delta^D(x'-y') (a_x a_{x'})^D \bar{\partial}_0^y \left[(\partial_0^x + 2DH a_x) K_{BB}(x; x) \right] i \Delta_A(x; x'), \quad (6.51)$$

where we used identity (6.27) applied to K_{BB} . Adding to this the $6b$ diagram, we can move the temporal derivatives inside, away from the external mode functions,

$$\begin{aligned} \left[-iV_{6a+b} \right]_{BB}^{\Delta\alpha} &= \frac{1}{2} (\kappa\lambda)^2 \delta^D(x-y) \delta^D(x'-y') (a_x a_{x'})^D \\ &\times (\partial_0^x + DH a_x) \left[(\partial_0^x + 2DH a_x) K_{BB}(x; x) \times i \Delta_A(x; x') \right]. \end{aligned} \quad (6.52)$$

The two remaining contributions are inferred by reflecting coordinates,

$$\begin{aligned} \left[-iV_{6c+d} \right]_{BB}^{\Delta\alpha} &= \frac{1}{2} (\kappa\lambda)^2 \delta^D(x-y) \delta^D(x'-y') (a_x a_{x'})^D \\ &\times (\partial_0^{x'} + DH a_{x'}) \left[i \Delta_A(x; x') \times (\partial_0^{x'} + 2DH a_{x'}) K_{BB}(x'; x') \right]. \end{aligned} \quad (6.53)$$

Diagram class 7. Here we just need two contractions (6.39) applied to (4.27) and (4.28) that immediately yield

$$\left[-iV_{7a} \right]_{BB}^{\Delta\alpha} = -(\kappa\lambda)^2 \delta^D(x-y) \delta^D(x'-y') (a_x a_{x'})^D \bar{\partial}_0^x \bar{\partial}_0^y \times K_{BB}(x; x) i \Delta_A(x; x'), \quad (6.54)$$

$$\left[-iV_{7b} \right]_{BB}^{\Delta\alpha} = -(\kappa\lambda)^2 \delta^D(x-y) \delta^D(x'-y') (a_x a_{x'})^D i \Delta_A(x; x') K_{BB}(x'; x') \times \bar{\partial}_0^{x'} \bar{\partial}_0^{y'}. \quad (6.55)$$

Cancellation of non-local contributions. Just as for the AA part, it is natural to group together contributions (6.40), (6.46), (6.48) and (6.49), as the non-local contributions cancel, and we are left with

$$\begin{aligned} & \left[-iV_{0a} - iV_{\overline{4a+b+c+d}} - iV_{\overline{5a+b+c+d}} \right]_{BB}^{\Delta\alpha} \\ &= i \int d^D z d^D z' [\partial_0^z i\Delta_A(x; z)] \left(\frac{K_{BB}(z; z')}{\mathcal{D}_z \delta^D(z-z')} \right) [\partial_0^{z'} i\Delta_A(z'; x')]. \end{aligned} \quad (6.56)$$

Applying here the same sequence of operations as we applied to Eq. (6.33) at end of the AA section, we get the remaining term to reduce to

$$\begin{aligned} & \left[-iV_{0a} - iV_{\overline{4a+b+c+d}} - iV_{\overline{5a+b+c+d}} \right]_{BB}^{\Delta\alpha} = (\kappa\lambda)^2 \delta^D(x-y) \delta^D(x'-y') (a_x a_{x'})^D \\ & \times \left\{ -i \int d^D z a_z^{D-2} [\partial_0^z i\Delta_A(x; z)] \times \left[(\partial_z \cdot \partial_{z'} - (D-2)H^2 a_z^2) K_{BB}(z; z') \right]_{z \rightarrow z'} \times [\partial_0^z i\Delta_A(z; x')] \right. \\ & \quad + \frac{1}{2} K_{BB}(x; x) \times [\partial_0^x + (D-2)H a_x] \partial_0^x i\Delta_A(x; x') \\ & \quad \quad + \frac{1}{2} [\partial_0^{x'} + (D-2)H a_{x'}] \partial_0^{x'} i\Delta_A(x; x') \times K_{BB}(x'; x') \\ & \quad \left. + \frac{1}{2} \partial_0^x K_{BB}(x; x) \times \partial_0^x i\Delta_A(x; x') + \frac{1}{2} \partial_0^{x'} K_{BB}(x'; x') \times \partial_0^{x'} i\Delta_A(x; x') \right\}. \end{aligned} \quad (6.57)$$

6.3 Final reduction

Having exploited derivative interactions to reduce the AA and BB parts of diagram classes 0–7, we managed to get all contributions to the form that require only the coincidence limits of integrated propagators K_{AA} and K_{BB} and their first two derivatives, that are given in (5.13)–(5.18). Now we substitute for these, keeping only the relevant logarithm terms, and bring the contributions from both parts together. All the final contributions are summarized in the first three rows of Table 2 in the concluding section.

Diagram classes 0–5. It is convenient to consider the first six diagram classes together. The total contribution from the $0b$ diagram comes from adding (6.6) and (6.41),

$$\left[-iV_{0b} \right]^{\Delta\alpha} = k(\kappa\lambda)^2 \delta^D(x-y) \delta^D(x'-y') (a_x a_{x'})^D \left[\frac{1}{2} D(D-1) Q_{AA}(x; x') - 2DL_{AA}(x; x') \right], \quad (6.58)$$

where

$$Q_{AA}(x; x') = -i \int d^D z a_z^{D-2} \ln(a_z) \partial_z^\mu i\Delta_A(x; z) \times \partial_\mu^z i\Delta_A(z; x'), \quad (6.59)$$

$$L_{AA}(x; x') = -i \int d^D z a_z^{D-2} \ln(a_z) \nabla_z^\mu i\Delta_A(x; z) \times \nabla_\mu^z i\Delta_A(z; x'), \quad (6.60)$$

are special cases of integrated propagators defined in (A.1) and (A.2) in Appendix A. Contributions from diagrams in class $\bar{1}$, given in (6.8), (6.9), (6.43), and (6.44), simply give

$$\left[-iV_{\overline{1b+c}} \right]^{\Delta\alpha} = k(\kappa\lambda)^2 \delta^D(x-y) \delta^D(x'-y') (a_x a_{x'})^D \times \frac{D(D-1)}{2} \ln(a_x a_{x'}) i\Delta_A(x; x'), \quad (6.61)$$

while the contributions from diagram $0a$ and classes $\bar{4}$ and $\bar{5}$, given in (6.36) and (6.57), combine into

$$\begin{aligned} & \left[-iV_{0a} - iV_{\bar{4}} - iV_{\bar{5}} \right]^{\Delta\alpha} = k(\kappa\lambda)^2 \delta^D(x-y) \delta^D(x'-y') (a_x a_{x'})^D \\ & \times \left\{ -\frac{D-1}{D-3} Q_{AA}(x; x') + \frac{(D-1)(D-2)}{D-3} L_{AA}(x; x') + \left[\frac{1}{D-3} \left(\frac{\ln(a_x)}{H a_x} \partial_0^x + \frac{\ln(a_{x'})}{H a_{x'}} \partial_0^{x'} \right) \right. \right. \end{aligned}$$

$$+ \frac{D-4}{2(D-3)} \left(\frac{\ln(a_x)}{H^2 a_x^2} \nabla_x^2 + \frac{\ln(a_{x'})}{H^2 a_{x'}^2} \nabla_{x'}^2 \right) + \frac{1}{2(D-3)} \left(\frac{\ln(a_x)}{H^2 a_x^D} \mathcal{D}_x + \frac{\ln(a_{x'})}{H^2 a_{x'}^D} \mathcal{D}_{x'} \right) \Big] i\Delta_A(x; x') \Big\}. \quad (6.62)$$

Upon using the identity that follows from the solutions (A.7) and (A.9) for integrated propagators,

$$(D-1)Q_{AA}(x; x') - 2L_{AA}(x; x') \longrightarrow \left(\frac{\ln(a_x)}{H a_x} \partial_0^x + \frac{\ln(a_{x'})}{H a_{x'}} \partial_0^{x'} \right) i\Delta_A(x; x'), \quad (6.63)$$

where we kept only the logarithm terms, the total contribution from diagrams 0–5 reads:

$$\begin{aligned} \left[-iV_{0-5} \right]^{\Delta\alpha} &= k(\kappa\lambda)^2 \delta^D(x-y) \delta^D(x'-y') (a_x a_{x'})^D \left[\frac{D(D-1)}{2} \ln(a_x a_{x'}) + \frac{D}{2} \left(\frac{\ln(a_x)}{H a_x} \partial_0^x + \frac{\ln(a_{x'})}{H a_{x'}} \partial_0^{x'} \right) \right. \\ &\quad \left. + \frac{D-4}{2(D-3)} \left(\frac{\ln(a_x)}{H^2 a_x^2} \nabla_x^2 + \frac{\ln(a_{x'})}{H^2 a_{x'}^2} \nabla_{x'}^2 \right) + \frac{1}{2(D-3)} \left(\frac{\ln(a_x)}{H^2 a_x^D} \mathcal{D}_x + \frac{\ln(a_{x'})}{H^2 a_{x'}^D} \mathcal{D}_{x'} \right) \right] i\Delta_A(x; x'). \end{aligned} \quad (6.64)$$

Diagram classes 6–7. The AA part of class 6 in (6.28) and (6.29) does not contribute anything on account of the spatial derivative acting on the coincidence limit of the integrated propagator. The entire result comes from the BB part in (6.52) and (6.53),

$$\begin{aligned} \left[-iV_6 \right]^{\Delta\alpha} &= k(\kappa\lambda)^2 \delta^D(x-y) \delta^D(x'-y') (a_x a_{x'})^D \\ &\quad \times \left[-\frac{(D-1)^2}{D-3} \ln(a_x a_{x'}) - \frac{D-1}{D-3} \left(\frac{\ln(a_x)}{H a_x} \partial_0^x + \frac{\ln(a_{x'})}{H a_{x'}} \partial_0^{x'} \right) \right] i\Delta_A(x; x'). \end{aligned} \quad (6.65)$$

The total contribution of class 7 is also easily obtained by substituting in the appropriate coincidence limits of integrated propagators into (6.31), (6.32), (6.54) and (6.55),

$$\begin{aligned} \left[-iV_7 \right]^{\Delta\alpha} &= k(\kappa\lambda)^2 \delta^D(x-y) \delta^D(x'-y') (a_x a_{x'})^D \\ &\quad \times \left[-\frac{D-4}{D-3} \left(\frac{\ln(a_x)}{H^2 a_x^2} \bar{\nabla}_x \cdot \bar{\nabla}_y + \frac{\ln(a_{x'})}{H^2 a_{x'}^2} \bar{\nabla}_{x'} \cdot \bar{\nabla}_{y'} \right) - \frac{1}{D-3} \left(\frac{\ln(a_x)}{H^2 a_x^2} \bar{\partial}_x \cdot \bar{\partial}_y + \frac{\ln(a_{x'})}{H^2 a_{x'}^2} \bar{\partial}_{x'} \cdot \bar{\partial}_{y'} \right) \right] i\Delta_A(x; x'). \end{aligned} \quad (6.66)$$

7 Reducing mode function corrections

In addition to the eight classes of diagrams considered in the preceding section, here we work out the contributions from the corrections to external mode functions. In what follows we will compute the two contributions (4.43) and (4.44) to the self-mass of the massive scalar, assuming that the tree-level mode function is connected to its y -leg, as appears in Eq. (4.45).

7.1 Preliminary reduction of AA parts

Reducing diagram I requires the same contraction (6.30) already worked out for diagram class 7. Dropping immediately the terms containing kinetic operators that annihilate the external mode function, we get

$$\left[-i\mathcal{M}_I^2 \right]_{AA}^{\Delta\alpha} = \kappa^2 \left[(\mathcal{D}_x - a_x^D m^2) (\bar{\nabla}_x \cdot \bar{\nabla}_y) + (\bar{\mathcal{D}}_x - a_x^D m^2) (\nabla_x \cdot \bar{\nabla}_y) \right] (\mathcal{D}_y - a_y^D m^2) \left(K_{AA}(x; y) \right) \left(i\Delta_m(x; y) \right). \quad (7.1)$$

The kinetic operator factored out acts on the massive propagator in the loop to create a delta function,

$$\left[-i\mathcal{M}_I^2 \right]_{AA}^{\Delta\alpha} = i\kappa^2 \left[(\mathcal{D}_x - a_x^D m^2) (\bar{\nabla}_x \cdot \bar{\nabla}_y) + (\bar{\mathcal{D}}_x - a_x^D m^2) (\nabla_x \cdot \bar{\nabla}_y) \right] \left(\frac{K_{AA}(x; y)}{\delta^D(x-y)} \right). \quad (7.2)$$

We then symmetrize the derivatives acting on the delta function in the first term using (6.34), and in the second term move the derivative away from the delta function,

$$\left[-i\mathcal{M}_I^2 \right]_{AA}^{\Delta\alpha} = -i\kappa^2 \left[(\bar{\nabla}_x \cdot \bar{\nabla}_y) (\partial_x \cdot \partial_y + a_x^2 m^2) \left(\frac{K_{AA}(x; y)}{a_x^{D-2} \delta^D(x-y)} \right) \right]$$

$$+ (\overline{\mathcal{D}}_x - a_x^D m^2) (\overline{\nabla}_x + \tilde{\nabla}_x) \cdot \overline{\nabla}_y \left(\frac{K_{AA}(x; y)}{\delta^D(x-y)} \right) \Big]. \quad (7.3)$$

Next, in the first term we integrate by parts the two derivatives away from the delta function, and in the second term we drop the spatial derivative of K_{AA} at coincidence,

$$\left[-i\mathcal{M}_I^2 \right]_{AA}^{\Delta\alpha} = -i\kappa^2 (\overline{\nabla}_x \cdot \overline{\nabla}_y) \left\{ a_x^{D-2} \left[(\overline{\partial}_x + \tilde{\partial}_x) \cdot (\overline{\partial}_y + \tilde{\partial}_y) + a_x^2 m^2 \right] + (\overline{\mathcal{D}}_x - a_x^D m^2) \right\} \left(\frac{K_{AA}(x; y)}{\delta^D(x-y)} \right). \quad (7.4)$$

For diagram *II* we need to contract the F-vertex into the tensor structure of the *AA* part of the graviton propagator, which produces the expression

$$\left[-i\mathcal{M}_{II}^2 \right]_{AA}^{\Delta\alpha} = i\kappa^2 a_x^{D-2} \left[(D-1) (\overline{\partial}_x \cdot \tilde{\partial}_x) (\overline{\partial}_y \cdot \tilde{\partial}_y) + (\overline{\nabla}_x \cdot \overline{\nabla}_y) (\tilde{\partial}_x \cdot \tilde{\partial}_y) \right. \\ \left. - \frac{1}{2} (D-1) (\overline{\partial}_x \cdot \overline{\partial}_y + a_x^2 m^2) (\tilde{\partial}_x \cdot \tilde{\partial}_y) \right] \left(\frac{K_{AA}(x; y)}{\delta^D(x-y)} \right), \quad (7.5)$$

that has the same structure as the expression (7.4) obtained for diagram *I*. Adding the two contributions (7.4) and (7.5) and substituting in the appropriate coincidence limits (5.13)–(5.15) then produces:

$$\left[-i\mathcal{M}_{I+II}^2 \right]_{AA}^{\Delta\alpha} = i\kappa^2 \delta^D(x-y) \ln(a_x) a_x^{D-2} \left\{ \left[\frac{\overline{\nabla}_x \cdot \overline{\nabla}_y}{H^2 a_x^2} + \frac{(D-1)^2}{2} \right] (\overline{\partial}_x \cdot \overline{\partial}_y + a_x^2 m^2) \right. \\ \left. + \frac{\overline{\nabla}_x \cdot \overline{\nabla}_y}{H^2 a_x^2} \left[a_x^{2-D} (\overline{\mathcal{D}}_x - a_x^D m^2) + H a_x (\overline{\partial}_0^x + \overline{\partial}_0^y) - (D-1) H^2 a_x^2 \right] \right\}. \quad (7.6)$$

7.2 Preliminary reduction of *BB* parts

For diagram *I* we require two contractions (6.39),

$$\left[-i\mathcal{M}_I^2 \right]_{BB}^{\Delta\alpha} = -\kappa^2 \left[(\mathcal{D}_x - a_x^D m^2) \overline{\partial}_0^x + (\overline{\mathcal{D}}_x - a_x^D m^2) \partial_0^x \right] (\mathcal{D}_y - a_y^D m^2) \overline{\partial}_0^y \left(\frac{K_{BB}(x; y)}{i\Delta_m(x; y)} \right), \quad (7.7)$$

where we immediately drop terms that annihilate the mode function. The factored out kinetic term pinches the massive propagator in the loop into a delta function,

$$\left[-i\mathcal{M}_I^2 \right]_{BB}^{\Delta\alpha} = -i\kappa^2 \left[\overline{\partial}_0^x \overline{\partial}_0^y (\mathcal{D}_x - a_x^D m^2) + \partial_0^x \overline{\partial}_0^y (\overline{\mathcal{D}}_x - a_x^D m^2) \right] \left(\frac{K_{BB}(x; y)}{\delta^D(x-y)} \right). \quad (7.8)$$

Using (6.34) we symmetrize the derivatives acting on the delta function in the first term,

$$\left[-i\mathcal{M}_I^2 \right]_{BB}^{\Delta\alpha} = i\kappa^2 \left[\overline{\partial}_0^x \overline{\partial}_0^y (\partial_x \cdot \partial_y + a_x^2 m^2) \left(\frac{K_{BB}(x; y)}{a_x^{D-2} \delta^D(x-y)} \right) \right. \\ \left. - \partial_0^x \overline{\partial}_0^y (\overline{\mathcal{D}}_x - a_x^D m^2) \left(\frac{K_{BB}(x; y)}{\delta^D(x-y)} \right) \right]. \quad (7.9)$$

We follow this by integrating by parts the derivatives away from the delta function in both terms, minding that here the order of operators matters,

$$\left[-i\mathcal{M}_I^2 \right]_{BB}^{\Delta\alpha} = i\kappa^2 \left\{ a_x^{D-2} \overline{\partial}_0^x \overline{\partial}_0^y \left[(\overline{\partial}_x + \tilde{\partial}_x) \cdot (\overline{\partial}_y + \tilde{\partial}_y) + a_x^2 m^2 \right] \right. \\ \left. + (\overline{\partial}_0^x + \tilde{\partial}_0^x) \overline{\partial}_0^y (\overline{\mathcal{D}}_x - a_x^D m^2) \right\} \left(\frac{K_{BB}(x; y)}{\delta^D(x-y)} \right). \quad (7.10)$$

For diagram *II* we need the contraction of the F-vertex into the tensor structure of the *BB* part of the graviton propagator,

$$\begin{aligned} \left[-i\mathcal{M}_{II}^2 \right]_{BB}^{\Delta\alpha} &= i\kappa^2 a_x^{D-2} \left\{ (\bar{\partial}_x \cdot \tilde{\partial}_x) (\bar{\partial}_y \cdot \tilde{\partial}_y) - \bar{\partial}_0^x \bar{\partial}_0^y (\tilde{\partial}_x \cdot \tilde{\partial}_y) + (D-4) H a_x \bar{\partial}_0^x (\bar{\partial}_y \cdot \tilde{\partial}_y) \right. \\ &\quad + (D-4) H a_y \bar{\partial}_0^y (\bar{\partial}_x \cdot \tilde{\partial}_x) + 2H a_x (\tilde{\partial}_0^x + (D-2) H a_x) (\bar{\partial}_x \cdot \bar{\partial}_y) \\ &\quad \left. - \frac{1}{2} \left[(\tilde{\partial}_x \cdot \tilde{\partial}_y) + (D-2) H a_x (\tilde{\partial}_0^x + \tilde{\partial}_0^y + D H a_x) \right] (\bar{\partial}_x \cdot \bar{\partial}_y + a_x^2 m^2) \right\} \left(\frac{K_{BB}(x; y)}{\delta^D(x-y)} \right). \end{aligned} \quad (7.11)$$

Collecting both contributions (7.10) and (7.11), and substituting in them the appropriate coincidence limits of K_{BB} then gives

$$\begin{aligned} \left[-i\mathcal{M}_{I+II}^2 \right]_{BB}^{\Delta\alpha} &= \frac{ik}{D-3} \kappa^2 \delta^D(y-x) \ln(a_x) a_x^{D-2} \left\{ \left[-\frac{1}{H^2 a_x^2} \bar{\partial}_0^x \bar{\partial}_0^y + \frac{(D-1)(D-3)}{2} \right] (\bar{\partial}_x \cdot \bar{\partial}_y + a_x^2 m^2) \right. \\ &\quad \left. - \frac{1}{H^2 a_x^2} (\bar{\partial}_0^x - H a_x) \bar{\partial}_0^y (\bar{\mathcal{D}}_x - a_x^D m^2) - \frac{1}{H a_x} (\bar{\partial}_0^x + \bar{\partial}_0^y - H a_x) \bar{\partial}_0^x \bar{\partial}_0^y - 2(D-3) \bar{\nabla}_x \cdot \bar{\nabla}_y \right\}. \end{aligned} \quad (7.12)$$

7.3 Final reduction

Adding the total *AA* contribution (7.6) and the total *BB* contribution (7.12) we have

$$\begin{aligned} \left[-i\mathcal{M}_{I+II}^2 \right]^{\Delta\alpha} &= \frac{ik\kappa^2}{D-3} \delta^D(x-y) \ln(a_x) a_x^{D-2} \left\{ \frac{1}{H^2 a_x^2} \left[\bar{\partial}_x \cdot \bar{\partial}_y + (D-4) \bar{\nabla}_x \cdot \bar{\nabla}_y + H a_x \bar{\partial}_0^y \right] (\bar{\mathcal{D}}_x - a_x^D m^2) \right. \\ &\quad + \frac{1}{H^2 a_x^2} \left[\bar{\partial}_x \cdot \bar{\partial}_y + (D-4) \bar{\nabla}_x \cdot \bar{\nabla}_y + \frac{D(D-1)(D-3)}{2} H^2 a_x^2 \right] (\bar{\partial}_x \cdot \bar{\partial}_y + a_x^2 m^2) \\ &\quad \left. + \frac{1}{H a_x} \left[\bar{\partial}_x \cdot \bar{\partial}_y + (D-4) \bar{\nabla}_x \cdot \bar{\nabla}_y \right] (\bar{\partial}_0^x + \bar{\partial}_0^y - H a_x) - D(D-3) \bar{\nabla}_x \cdot \bar{\nabla}_y \right\}. \end{aligned} \quad (7.13)$$

Further reduction is possible using the following identities in which we keep only the logarithm terms,

$$\delta^D(x-y) \ln(a_x) a_x^{D-3} (\bar{\partial}_0^x + \bar{\partial}_0^y) \longrightarrow -(D-3) H \delta^D(x-y) \ln(a_x) a_x^{D-2}, \quad (7.14)$$

$$\begin{aligned} \delta^D(x-y) \ln(a_x) a_x^{D-2} (\bar{\partial}_x \cdot \bar{\partial}_y + a_x^2 m^2) \\ \longrightarrow -\frac{1}{2} \delta^D(x-y) \ln(a_x) \left[(\bar{\mathcal{D}}_x - a_x^D m^2) + (\bar{\mathcal{D}}_y - a_y^D m^2) \right], \end{aligned} \quad (7.15)$$

$$\begin{aligned} \delta^D(x-y) \ln(a_x) a_x^{D-4} (\bar{\partial}_x \cdot \bar{\partial}_y + a_x^2 m^2) \\ \longrightarrow \delta^D(x-y) \ln(a_x) \left[(D-3) H^2 a_x^{D-2} - \frac{1}{2a_x^2} (\bar{\mathcal{D}}_x - a_x^D m^2) - \frac{1}{2a_y^2} (\bar{\mathcal{D}}_y - a_y^D m^2) \right], \end{aligned} \quad (7.16)$$

that follow from the second vertex identity (3.5). Being careful about the non-commuting derivatives when applying them produces

$$\begin{aligned} \left[-i\mathcal{M}_{I+II}^2 \right]^{\Delta\alpha} &= ik\kappa^2 \delta^D(x-y) \ln(a_x) \frac{1}{(D-3)H^2 a_x^2} \left\{ -\frac{1}{2} \left[(\bar{\mathcal{D}}_x - a_x^D m^2) + (\bar{\mathcal{D}}_y - a_y^D m^2) \right] \bar{\partial}_x \cdot \bar{\partial}_y \right. \\ &\quad + \left[\bar{\partial}_x \cdot \bar{\partial}_y + \frac{D-4}{2} \bar{\nabla}_x \cdot \bar{\nabla}_y + H a_x \bar{\partial}_0^y - \frac{D(D-1)(D-3)}{4} \right] (\bar{\mathcal{D}}_x - a_x^D m^2) \\ &\quad \left. - H^2 a_x^D \left[\bar{\partial}_x \cdot \bar{\partial}_y + (D^2 - 2D - 4) \bar{\nabla}_x \cdot \bar{\nabla}_y \right] \right\}. \end{aligned} \quad (7.17)$$

Next we use the commutation identity (3.7) on the term in the first line,

$$\begin{aligned} \left[-i\mathcal{M}_{I+II}^2 \right]^{\Delta\alpha} &= ik\kappa^2 \delta^D(x-y) \ln(a_x) \frac{1}{(D-3)H^2 a_x^2} \left\{ \frac{1}{2} \left[\bar{\partial}_x \cdot \bar{\partial}_y + (D-4) \bar{\nabla}_x \cdot \bar{\nabla}_y - (D-4) H a_x \bar{\partial}_0^y \right. \right. \\ &\quad \left. \left. - \frac{D(D-1)(D-3)}{2} H^2 a_x^2 \right] (\bar{\mathcal{D}}_x - a_x^D m^2) - H^2 a_x^D \left[(D-1) \bar{\partial}_x \cdot \bar{\partial}_y + (D^2 - 3D - 2) \bar{\nabla}_x \cdot \bar{\nabla}_y \right] \right. \\ &\quad \left. + H a_x^{D+1} m^2 (\bar{\partial}_0^x + \bar{\partial}_0^y) \right\}. \end{aligned} \quad (7.18)$$

This is followed by applying the identity (A.13) from Appendix A, in which we keep only the logarithm terms,

$$\delta^D(x-y) \ln(a_x) a_x^{D-2} \bar{\nabla}_x \cdot \bar{\nabla}_y \longrightarrow \delta^D(x-y) \ln(a_x) \times \frac{-1}{2Ha_x} \left[\bar{\partial}_0^y + \frac{D-1}{2} Ha_y \right] (\bar{\mathcal{D}}_x - a_x^D m^2), \quad (7.19)$$

and by once more using (7.14) and (7.15), which finally produces

$$\left[-i\mathcal{M}_{I+II}^2 \right]^{\Delta\alpha} = \delta^D(x-y) \frac{ik\kappa^2 \ln(a_x)}{2(D-3)H^2 a_x^2} \left[\bar{\partial}_x \cdot \bar{\partial}_y + (D-4) \bar{\nabla}_x \cdot \bar{\nabla}_y + (D^2 - 4D + 2) Ha_x \bar{\partial}_0^y \right] (\bar{\mathcal{D}}_x - a_x^D m^2). \quad (7.20)$$

From here we can simply read off the solution for the mode function correction by stripping the last kinetic operator,

$$\delta u_{I+II}(x) = -\frac{k\kappa^2 \ln(a_x)}{2(D-3)H^2 a_x^2} \left[\bar{\partial}_x \cdot \partial_x + (D-4) \bar{\nabla}_x \cdot \nabla_x + (D^2 - 4D + 2) Ha_x \partial_0^x \right] u(x), \quad (7.21)$$

where we dropped the homogeneous parts that do not contain logarithms. The barred derivatives in this expression are assumed to act on the remainder of the diagrams in (4.39)–(4.42) that the mode function correction attaches to.

7.4 Contribution to effective self-mass

We now connect the $\Delta\alpha$ variation of the one-loop mode function correction to the main body of the diagram according to (4.39)–(4.42). The resulting expressions give local vertex corrections with the topology of middle two diagrams on the right-hand side of (3.3), and can thus be written using the same conventions as for the 4-point diagrams introduced at the beginning of Sec. 4,

$$\left[-iV_{I+II,a} \right]^{\Delta\alpha} = k(\kappa\lambda)^2 \delta^D(x-y) \delta^D(x'-y') (a_x a_{x'})^D \frac{\ln(a_x)}{2(D-3)H^2 a_x^2} \left[\bar{\partial}_y \cdot (\bar{\partial}_x + \partial_x) + (D-4) \bar{\nabla}_y \cdot (\bar{\nabla}_x + \nabla_x) + (D^2 - 5D + 2) Ha_x \bar{\partial}_0^y \right] i\Delta_A(x; x'), \quad (7.22)$$

$$\left[-iV_{I+II,b} \right]^{\Delta\alpha} = k(\kappa\lambda)^2 \delta^D(x-y) \delta^D(x'-y') (a_x a_{x'})^D \frac{\ln(a_x)}{2(D-3)H^2 a_x^2} \left[\bar{\partial}_x \cdot (\bar{\partial}_y + \partial_x) + (D-4) \bar{\nabla}_x \cdot (\bar{\nabla}_y + \nabla_x) + (D^2 - 5D + 2) Ha_x \bar{\partial}_0^x \right] i\Delta_A(x; x'), \quad (7.23)$$

$$\left[-iV_{I+II,c} \right]^{\Delta\alpha} = k(\kappa\lambda)^2 \delta^D(x-y) \delta^D(x'-y') (a_x a_{x'})^D \frac{\ln(a_{x'})}{2(D-3)H^2 a_{x'}^2} \left[\bar{\partial}_{y'} \cdot (\bar{\partial}_{x'} + \partial_{x'}) + (D-4) \bar{\nabla}_{y'} \cdot (\bar{\nabla}_{x'} + \nabla_{x'}) + (D^2 - 5D + 2) Ha_{x'} \bar{\partial}_0^{y'} \right] i\Delta_A(x; x'), \quad (7.24)$$

$$\left[-iV_{I+II,d} \right]^{\Delta\alpha} = k(\kappa\lambda)^2 \delta^D(x-y) \delta^D(x'-y') (a_x a_{x'})^D \frac{\ln(a_{x'})}{2(D-3)H^2 a_{x'}^2} \left[\bar{\partial}_{x'} \cdot (\bar{\partial}_{y'} + \partial_{x'}) + (D-4) \bar{\nabla}_{x'} \cdot (\bar{\nabla}_{y'} + \nabla_{x'}) + (D^2 - 5D + 2) Ha_{x'} \bar{\partial}_0^{x'} \right] i\Delta_A(x; x'). \quad (7.25)$$

Therefore, these contributions will combine with the contributions worked out in Sec. 6, but should be further reduced before that.

The reduction can be pursued after combining a and b contributions,

$$\left[-iV_{I+II,a+b} \right]^{\Delta\alpha} = k(\kappa\lambda)^2 \delta^D(x-y) \delta^D(x'-y') (a_x a_{x'})^D \frac{\ln(a_x)}{(D-3)H^2 a_x^2} \left[\bar{\partial}_x \cdot \bar{\partial}_y + (D-4) \bar{\nabla}_x \cdot \bar{\nabla}_y + \frac{1}{2} (\bar{\partial}_x + \bar{\partial}_y) \cdot \partial_x + \frac{1}{2} (D-4) (\bar{\nabla}_x + \bar{\nabla}_y) \cdot \nabla_x + \frac{D^2 - 5D + 2}{2} Ha_x (\bar{\partial}_0^x + \bar{\partial}_0^y) \right] i\Delta_A(x; x'). \quad (7.26)$$

This allows us to reflect the derivatives in the second line away from the external mode functions, which produces the final result,

$$\left[-iV_{I+II,a+b} \right]^{\Delta\alpha} = k(\kappa\lambda)^2 \delta^D(x-y) \delta^D(x'-y') (a_x a_{x'})^D \frac{\ln(a_x)}{(D-3)H^2 a_x^2} \left[\bar{\partial}_x \cdot \bar{\partial}_y + (D-4) \bar{\nabla}_x \cdot \bar{\nabla}_y \right]$$

$$- \frac{1}{2a_x^{D-2}} \mathcal{D}_x - \frac{D-4}{2} \nabla_x^2 - \frac{D^2-5D+2}{2} H a_x \partial_0^x - \frac{(D-1)(D^2-5D+2)}{2} H^2 a_x^2 \Big] i \Delta_A(x; x'), \quad (7.27)$$

The c and d contributions combine in an analogous way,

$$\begin{aligned} \left[-iV_{I+II,c+d} \right]^{\Delta\alpha} &= k(\kappa\lambda)^2 \delta^D(x-y) \delta^D(x'-y') (a_x a_{x'})^D \frac{\ln(a_{x'})}{(D-3)H^2 a_{x'}^2} \left[\bar{\partial}_{x'} \cdot \bar{\partial}_{y'} + (D-4) \bar{\nabla}_{x'} \cdot \bar{\nabla}_{y'} \right. \\ &\quad \left. - \frac{1}{2a_{x'}^{D-2}} \mathcal{D}_{x'} - \frac{D-4}{2} \nabla_{x'}^2 - \frac{D^2-5D+2}{2} H a_{x'} \partial_0^{x'} - \frac{(D-1)(D^2-5D+2)}{2} H^2 a_{x'}^2 \right] i \Delta_A(x; x'). \end{aligned} \quad (7.28)$$

Adding these contributions to the ones worked out in Sec. 6 produces a vanishing result for the $\Delta\alpha$ variation of the effective self-mass, as summarized by Table 2 in the following section.

8 Discussion and conclusions

In this work we set out to test the gauge-independence of our program for purging gauge dependence from effective field equations, which was set up with the goal of obtaining physical predictions for quantum-gravitational effects during inflation. The central objection to the standard procedure—quantum-correcting effective field equations using the 1PI two-point function—is that the 1PI two-point function depends on the graviton gauge. We contend that this dependence arises because one typically neglects quantum-gravitational corrections associated with the source and the observer, which in our setup are represented by a massive matter field, which acts both as a source and as an observer, in close analogy with how gauge-independence is achieved for the flat-space S-matrix.

We consider the system in (2.1), consisting of a heavy scalar interacting through the exchange of a massless minimally coupled (MMC) scalar on a de Sitter background, and we incorporate source and observer corrections by forming the position-space amplitudes corresponding to t -channel scattering. These amplitudes receive contributions from the 1PI two-, three-, and four-point functions, as depicted by the skeleton expansion in (3.11). In addition, as we uncovered here, one must also include one-loop corrections to the external mode functions, which are captured by the 1PI two-point function of the massive field. Our strategy is to reduce the full set of diagrams to the four topologies shown in (3.3), exploiting the derivative structure of gravitational interactions and, when needed, applying the Donoghue identities [38–40, 45] to isolate the relevant terms. Upon inserting the exchange propagators using Eq. (3.8), these reduced topologies can be interpreted as corrections to the 1PI two-point function of the MMC scalar. This effective correction is conjectured to be gauge-independent and can therefore be used to quantum-correct the field equations and extract physical predictions for quantum-gravitational effects. In flat space this program was implemented and the resulting effective 1PI two-point function was verified to be gauge independent for one-graviton-loop corrections to an MMC scalar [36] and to electromagnetism [46]. The present work examines gauge dependence of the analogous construction on a de Sitter background.

In order to test gauge dependence in de Sitter, we computed the contribution to the effective self-mass induced by the part of the de Sitter-breaking graviton propagator [47] that depends on one of the two infinitesimal gauge-fixing parameters. This defines a one-parameter subfamily of gauges for which the dependence on the gauge-fixing parameter is linear, and hence can be extended to finite values [48]. We refer to this component of the graviton propagator defined in Eq. (5.10), and to the contributions it generates, as the $\Delta\alpha$ variations.

In Secs. 6 and 7 we computed the $\Delta\alpha$ variations of the diagrams listed in Sec. 4. After reducing all contributions to the topologies on the right-hand side of (3.3), which required no Donoghue identities and was achieved by judicious integrations by parts, the full result takes the form

$$\left[-iV \right]^{\Delta\alpha} = k(\kappa\lambda)^2 \delta^D(x-y) \delta^D(x'-y') (a_x a_{x'})^D \left[C_1 \ln(a_x a_{x'}) + C_2 \left(\frac{\ln(a_x)}{H a_x} \partial_0^x + \frac{\ln(a_{x'})}{H a_{x'}} \partial_0^{x'} \right) \right]$$

$$\begin{aligned}
& + C_3 \left(\frac{\ln(a_x)}{H^2 a_x^2} \nabla_x^2 + \frac{\ln(a_{x'})}{H^2 a_{x'}^2} \nabla_{x'}^2 \right) + C_4 \left(\frac{\ln(a_x)}{H^2 a_x^2} \nabla_x \cdot \nabla_y + \frac{\ln(a_{x'})}{H^2 a_{x'}^2} \nabla_{x'} \cdot \nabla_{y'} \right) \\
& + C_5 \left(\frac{\ln(a_x)}{H^2 a_x^2} \bar{\partial}_x \cdot \bar{\partial}_y + \frac{\ln(a_{x'})}{H^2 a_{x'}^2} \bar{\partial}_{x'} \cdot \bar{\partial}_{y'} \right) + C_6 \left(\frac{\ln(a_x)}{H^2 a_x^D} \mathcal{D}_x + \frac{\ln(a_{x'})}{H^2 a_{x'}^D} \mathcal{D}_{x'} \right) \Big] i\Delta_A(x; x'). \quad (8.1)
\end{aligned}$$

This expression contains five contributions with local corrections to the vertices, parametrized by the coefficients C_1 – C_5 , and one ultra-local contribution, parametrized by C_6 , which involves the kinetic operator that pinches the MMC scalar propagator. The contributions from the different diagram classes to these coefficients are summarized in Table 2, which shows that they all cancel. This is the main result of our paper: the $\Delta\alpha$ variation drops out from the final one-

	C_1	C_2	C_3	C_4	C_5	C_6
0–5	$\frac{D(D-1)}{2}$	$\frac{D}{2}$	$\frac{D-4}{2(D-3)}$	0	0	$\frac{1}{2(D-3)}$
6	$-\frac{(D-1)^2}{D-3}$	$-\frac{D-1}{D-3}$	0	0	0	0
7	0	0	0	$-\frac{D-4}{D-3}$	$-\frac{1}{D-3}$	0
δu	$\frac{(D-1)^2}{D-3} - \frac{D(D-1)}{2}$	$\frac{D-1}{D-3} - \frac{D}{2}$	$-\frac{D-4}{2(D-3)}$	$\frac{D-4}{D-3}$	$\frac{1}{D-3}$	$-\frac{1}{2(D-3)}$
Total	0	0	0	0	0	0

Table 2: Contributions to coefficients in the final expression (8.1) for the $\Delta\alpha$ gauge variation of the effective self-mass, coming from different diagrams worked out in Secs. 6 and 7.

graviton-loop correction to the effective scalar self-mass. The cancellation is highly non-trivial and occurs only after including contributions from *all* diagram classes and *all* external mode function corrections. This situation is considerably more intricate than in flat space [36], where diagrams from classes 6 and 7 vanish identically, and where diagrams from classes *I* and *II* do not contribute to field-strength renormalization.

The cancellation of the $\Delta\alpha$ variation reported here is compelling and strengthens confidence in our program for constructing gauge-independent quantum-corrected effective field equations in a cosmological setting. At the same time, it completes only half of the overall gauge test: the graviton propagator of [47] also depends on a second gauge-fixing parameter β , whose infinitesimal variation around unity we denote by $\delta\beta$. Demonstrating that the $\delta\beta$ variation also cancels between all the diagrams should establish gauge-independence of the effective self-mass at the same level as was accomplished in flat space [36]. We also hope that by performing the computation of the $\delta\beta$ variation we will be able to test our de Sitter generalizations of the Donoghue identities made in [49], and also to understand whether any of the additional diagrams collected in Appendix B can contribute to the MMC scalar exchange potential.

Finally, it will be necessary to update the computation of the tentative gauge-independent contribution to the MMC scalar self-mass reported in [49]. The key lesson of the present work is that the additional diagram classes 6 and 7, together with the external mode-function corrections represented by classes *I* and *II*, are essential for canceling gauge dependence, and therefore must also be included when extracting the gauge-independent part. Only once this is done will we have a definitive answer as to whether the large quantum-gravitational logarithms persist in the exchange potential mediated by the MMC scalar.

Acknowledgments

The authors acknowledge a generous support by the Delta ITP consortium, a program of the Netherlands Organisation for Scientific Research (NWO) that is funded by the Dutch Ministry of Education, Culture and Science (OCW) - NWO project number 24.001.027. DG was supported by the Czech Science Foundation (GAČR) grant 24-13079S. SPM was partially supported by Taiwan NSTC grants 113-2112-M-006-013 and 114-2112-M-006-020. TP is supported by the NWA ORC 2023 consortium grant: Cosmic emergence: from abstract simplicity to complex diversity (Kosmische emergentie: van abstracte eenvoud naar complexe diversiteit) and by The Magnetic Universe NWO grant OCENW.XL.23.147. RPW was partially supported by NSF grant PHY-2207514 and by the Institute for Fundamental Theory at the University of Florida.

A Integrated propagators

In Sec. 6.3 we need expressions for two integrated propagators,

$$Q_{\nu\nu}(x; x') = -i \int d^D z a_z^{D-2} \ln(a_z) \left[\partial_z^\mu i\Delta_\nu(x; z) \partial_\mu^z i\Delta_\nu(z; x') + a_z^2 M_\nu^2 i\Delta_\nu(x; z) i\Delta_\nu(z; x') \right], \quad (\text{A.1})$$

$$L_{\nu\nu}(x; x') = -i \int d^D z a_z^{D-2} \ln(a_z) \nabla_z^\mu i\Delta_\nu(x; z) \nabla_\mu^z i\Delta_\nu(z; x'), \quad (\text{A.2})$$

where the parameter ν is related to the mass of the propagators as

$$\nu^2 = \left(\frac{D-1}{2} \right)^2 - \frac{M_\nu^2}{H^2}, \quad (\text{A.3})$$

so that propagators in the integrands satisfy the equation of motion

$$(\mathcal{D}_x - a_x^D M_\nu^2) i\Delta_\nu(x; x') = i\delta^D(x-x'). \quad (\text{A.4})$$

Consequently, the integrated propagators in (A.1) and (A.2) satisfy sourced equations of motion,

$$(\mathcal{D}_x - a_x^D M_\nu^2) Q_{\nu\nu}(x; x') = -\ln(a_x) i\delta^D(x-x') + H a_x^{D-1} \partial_0^x i\Delta_\nu(x; x'), \quad (\text{A.5})$$

$$(\mathcal{D}_x - a_x^D M_\nu^2) L_{\nu\nu}(x; x') = -\ln(a_x) a_x^{D-2} \nabla_x^2 i\Delta_\nu(x; x'), \quad (\text{A.6})$$

with analogous equations satisfied on the primed coordinate.

The first of the two integrated propagators can be evaluated straightforwardly using the vertex identity (3.5), where the logarithm insertion is treated as the third leg of the vertex,

$$Q_{\nu\nu}(x; x') = -\frac{1}{2}(D-1)H^2 I_{\nu\nu}(x; x') - \frac{1}{2} \ln(a_x a_{x'}) i\Delta_\nu(x; x'), \quad (\text{A.7})$$

where the result includes an integrated propagator without any derivatives or logarithms in the integrand,

$$I_{\nu\nu}(x; x') = -i \int d^D z a_z^D i\Delta_\nu(x; z) i\Delta_\nu(z; x'). \quad (\text{A.8})$$

Evaluating the second integrated propagator (A.2) is not as straightforward. It is best dealt with in momentum space representation, using identities for the mode functions (see e.g. [48]). These allow to derive the following result,

$$\begin{aligned} L_{\nu\nu}(x; x') = & -\nu^2 H^2 I_{\nu\nu}(x; x') - \frac{\ln(a_x)+1}{2H a_x} \left[\partial_0^x + \frac{D-1}{2} H a_x \right] i\Delta_\nu(x; x') \\ & - \frac{\ln(a_{x'})+1}{2H a_{x'}} \left[\partial_0^{x'} + \frac{D-1}{2} H a_{x'} \right] i\Delta_\nu(x; x') + \frac{1}{2} i\Delta_\nu(x; x'). \end{aligned} \quad (\text{A.9})$$

It is sufficient to check that this identity satisfies the correct equation of motion (A.6), which is accomplished by applying the kinetic operator from the left hand-side of (A.6), and commuting it over derivatives and functions of the scale factor to obtain the right-hand side of (A.6).

In Sec. 7.3 we need another integrated propagator-like expression,

$$\bar{L}_\nu(x) = -i \int d^D z a_z^{D-2} \left[\ln(a_z) \nabla_\mu^z i \Delta_\nu(x; z) \times \nabla_z^\mu u_\nu(z) + \nu^2 a_z^2 H^2 i \Delta_\nu(x; z) u_\nu(z) \right], \quad (\text{A.10})$$

where $u_\nu(x)$ is a mode function satisfying a homogeneous equation,

$$(\mathcal{D}_x - a_x^D M_\nu^2) u_\nu(x) = 0. \quad (\text{A.11})$$

This integrated quantity satisfies the equation of motion

$$(\mathcal{D}_x - a_x^D M_\nu^2) \bar{L}_\nu(x) = a_x^{D-2} \left[-\ln(a_x) \nabla_x^2 + \nu^2 a_x^2 H^2 \right] u_\nu(x). \quad (\text{A.12})$$

We can guess the form of the solution based on the similarity of equation (A.12) with the equation in (A.6), whose solution we have found in (A.9). Up to a homogeneous part that we do not need, the solution reads

$$\bar{L}_\nu(x) = -\frac{\ln(a_x) + 1}{2H a_x} \left[\partial_0^x + \frac{D-1}{2} H a_x \right] u_\nu(x). \quad (\text{A.13})$$

It is sufficient to show that this expression satisfies the equation of motion (A.12), which requires applying the same steps as when proving that (A.9) satisfies its equation of motion.

B Additional diagrams

In addition to the diagrams in Fig. 1 representing the 4-point function corrections, for which we computed the $\Delta\alpha$ variation, there are several more classes of t -channel diagrams that contribute at the same perturbative order $(\kappa\lambda)^2$; these are classes depicted in Figs. 4. Even though they

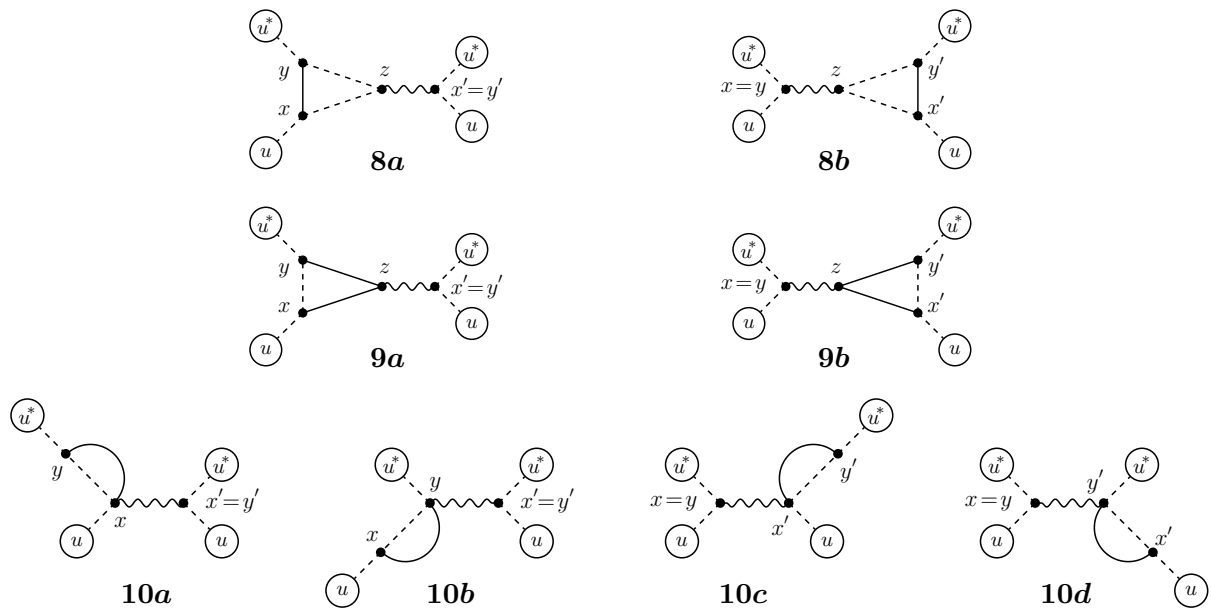


Figure 4: Three additional classes of diagrams that contribute at the same order $(\kappa\lambda)^2$ to the t -channel 4-point function.

naively seem to be corrections to the gravitational potential, rather than the scalar one, we should

be careful about making that conclusion prematurely. In fact, already in flat space obtaining the gauge-independent vacuum polarization required an analogue of one class of these diagrams [46]. Nonetheless, the $\Delta\alpha$ variations of these additional diagrams all vanish individually. This is due to the presence of vertex B that connects two external mode functions to the graviton mediating the interaction. By virtue of contractions (6.3) and (6.39), and the tree-level equation of motion (3.14) for the mode function, this always gives zero.

In addition, we should also list the mode function corrections in diagrams that naively look like the t -channel graviton exchange, that contribute at the same order,

$$\text{Diagram 1} + \text{Diagram 2} + \text{Diagram 3} + \text{Diagram 4} \quad (\text{B.1})$$

The mode function corrections for these diagrams are sourced by the massive scalar self-mass with loop corrections engendered by its interactions with the massless scalar, given in Fig 5.



Figure 5: One-loop diagrams correcting the self-mass of the massive scalar from the interaction with the massless scalar: the 3-vertex diagram (III) and the 4-vertex diagram (IV).

References

- [1] L. Parker, “Particle creation in expanding universes,” *Phys. Rev. Lett.* **21** (1968), 562-564
- [2] V. F. Mukhanov and G. V. Chibisov, “Quantum Fluctuations and a Nonsingular Universe,” *JETP Lett.* **33** (1981), 532-535
- [3] A. A. Starobinsky, “Spectrum of relict gravitational radiation and the early state of the universe,” *JETP Lett.* **30** (1979), 682-685
- [4] Y. Akrami *et al.* [Planck], “Planck 2018 results. X. Constraints on inflation,” *Astron. Astrophys.* **641** (2020), A10 [arXiv:1807.06211 [astro-ph.CO]].
- [5] J. F. Donoghue, “General relativity as an effective field theory: The leading quantum corrections,” *Phys. Rev. D* **50** (1994), 3874-3888 [arXiv:gr-qc/9405057 [gr-qc]].
- [6] J. F. Donoghue, “Introduction to the effective field theory description of gravity,” [arXiv:gr-qc/9512024 [gr-qc]].
- [7] C. P. Burgess, “Quantum gravity in everyday life: General relativity as an effective field theory,” *Living Rev. Rel.* **7** (2004), 5-56 [arXiv:gr-qc/0311082 [gr-qc]].
- [8] J. F. Donoghue, “The effective field theory treatment of quantum gravity,” *AIP Conf. Proc.* **1483** (2012) no.1, 73-94 [arXiv:1209.3511 [gr-qc]].
- [9] J. Donoghue, “Quantum gravity as a low energy effective field theory,” *Scholarpedia* **12** (2017) no.4, 32997

- [10] J. F. Donoghue, “Quantum General Relativity and Effective Field Theory,” in Handbook of Quantum Gravity, C. Bambi, L. Modesto and I. Shapiro, Springer, Singapore (2023) [arXiv:2211.09902 [hep-th]].
- [11] S. Boran, E. O. Kahya and S. Park, “One loop corrected conformally coupled scalar mode equations during inflation,” Phys. Rev. D **96** (2017) no.10, 105003 [erratum: Phys. Rev. D **98** (2018) no.2, 029903] [arXiv:1708.01831 [gr-qc]].
- [12] D. Glavan, S. P. Miao, T. Prokopec and R. P. Woodard, “One-loop Graviton Corrections to Conformal Scalars on a de Sitter Background,” Phys. Rev. D **103** (2021) no.10, 105022 [arXiv:2007.10395 [gr-qc]].
- [13] S. P. Miao and R. P. Woodard, “Gravitons Enhance Fermions during Inflation,” Phys. Rev. D **74** (2006), 024021 [arXiv:gr-qc/0603135 [gr-qc]].
- [14] D. Glavan, S. P. Miao, T. Prokopec and R. P. Woodard, “Electrodynamic Effects of Inflationary Gravitons,” Class. Quant. Grav. **31** (2014), 175002 [arXiv:1308.3453 [gr-qc]].
- [15] C. L. Wang and R. P. Woodard, “Excitation of Photons by Inflationary Gravitons,” Phys. Rev. D **91** (2015) no.12, 124054 [arXiv:1408.1448 [gr-qc]].
- [16] L. Tan, N. C. Tsamis and R. P. Woodard, “How inflationary gravitons affect gravitational radiation,” Phil. Trans. Roy. Soc. Lond. A **380** (2021), 0187 [arXiv:2107.13905 [gr-qc]].
- [17] D. Glavan, S. P. Miao, T. Prokopec and R. P. Woodard, “Large logarithms from quantum gravitational corrections to a massless, minimally coupled scalar on de Sitter,” JHEP **03** (2022), 088 [arXiv:2112.00959 [gr-qc]].
- [18] L. Tan, N. C. Tsamis and R. P. Woodard, “How Inflationary Gravitons Affect the Force of Gravity,” Universe **8** (2022) no.7, 376 [arXiv:2206.11467 [gr-qc]].
- [19] S. P. Miao, N. C. Tsamis and R. P. Woodard, “Summing inflationary logarithms in nonlinear sigma models,” JHEP **03** (2022), 069 [arXiv:2110.08715 [gr-qc]].
- [20] D. Glavan, S. P. Miao, T. Prokopec and R. P. Woodard, “Explaining large electromagnetic logarithms from loops of inflationary gravitons,” JHEP **08** (2023), 195 [arXiv:2307.09386 [gr-qc]].
- [21] N. C. Tsamis and R. P. Woodard, “The Structure of perturbative quantum gravity on a De Sitter background,” Commun. Math. Phys. **162** (1994), 217-248
- [22] R. P. Woodard, “de Sitter breaking in field theory,” published in “Deserfest: A Celebration of the Life and Works of Stanley Deser” (Eds. J. T. Liu, M. J. Duff, K. S. Stelle, R. P. Woodard), World Scientific (2006), [arXiv:gr-qc/0408002 [gr-qc]].
- [23] N. C. Tsamis and R. P. Woodard, “One loop graviton selfenergy in a locally de Sitter background,” Phys. Rev. D **54** (1996), 2621-2639 [arXiv:hep-ph/9602317 [hep-ph]].
- [24] S. P. Miao and R. P. Woodard, “The Fermion self-energy during inflation,” Class. Quant. Grav. **23** (2006), 1721-1762 [arXiv:gr-qc/0511140 [gr-qc]].
- [25] E. O. Kahya and R. P. Woodard, “Quantum Gravity Corrections to the One Loop Scalar Self-Mass during Inflation,” Phys. Rev. D **76** (2007), 124005 [arXiv:0709.0536 [gr-qc]].
- [26] S. P. Miao, “Quantum Gravitational Effects on Massive Fermions during Inflation I,” Phys. Rev. D **86** (2012), 104051 [arXiv:1207.5241 [gr-qc]].

- [27] K. E. Leonard and R. P. Woodard, “Graviton Corrections to Vacuum Polarization during Inflation,” *Class. Quant. Grav.* **31** (2014), 015010 [arXiv:1304.7265 [gr-qc]].
- [28] D. Glavan, S. P. Miao, T. Prokopec and R. P. Woodard, “Single graviton loop contribution to the self-mass of a massless, conformally coupled scalar on a de Sitter background,” *Phys. Rev. D* **101** (2020) no.10, 106016 [arXiv:2003.02549 [gr-qc]].
- [29] A. Higuchi, D. Marolf and I. A. Morrison, “de Sitter invariance of the dS graviton vacuum,” *Class. Quant. Grav.* **28** (2011), 245012 [arXiv:1107.2712 [hep-th]].
- [30] S. P. Miao, N. C. Tsamis and R. P. Woodard, “Gauging away Physics,” *Class. Quant. Grav.* **28** (2011), 245013 [arXiv:1107.4733 [gr-qc]].
- [31] I. A. Morrison, “On cosmic hair and ”de Sitter breaking” in linearized quantum gravity,” [arXiv:1302.1860 [gr-qc]].
- [32] S. P. Miao, P. J. Mora, N. C. Tsamis and R. P. Woodard, “Perils of analytic continuation,” *Phys. Rev. D* **89** (2014) no.10, 104004 [arXiv:1306.5410 [gr-qc]].
- [33] P. J. Mora, N. C. Tsamis and R. P. Woodard, “Graviton Propagator in a General Invariant Gauge on de Sitter,” *J. Math. Phys.* **53** (2012), 122502 [arXiv:1205.4468 [gr-qc]].
- [34] D. Glavan, S. P. Miao, T. Prokopec and R. P. Woodard, “Graviton Loop Corrections to Vacuum Polarization in de Sitter in a General Covariant Gauge,” *Class. Quant. Grav.* **32** (2015) no.19, 195014 [arXiv:1504.00894 [gr-qc]].
- [35] D. Glavan, S. P. Miao, T. Prokopec and R. P. Woodard, “One loop graviton corrections to dynamical photons in de Sitter,” *Class. Quant. Grav.* **34** (2017) no.8, 085002 [arXiv:1609.00386 [gr-qc]].
- [36] S. P. Miao, T. Prokopec and R. P. Woodard, “Deducing Cosmological Observables from the S-matrix,” *Phys. Rev. D* **96** (2017) no.10, 104029 [arXiv:1708.06239 [gr-qc]].
- [37] K. E. Leonard and R. P. Woodard, “Graviton Corrections to Maxwell’s Equations,” *Phys. Rev. D* **85** (2012), 104048 [arXiv:1202.5800 [gr-qc]].
- [38] J. F. Donoghue, “Leading quantum correction to the Newtonian potential,” *Phys. Rev. Lett.* **72** (1994), 2996-2999 [arXiv:gr-qc/9310024 [gr-qc]].
- [39] N. E. J. Bjerrum-Bohr, “Leading quantum gravitational corrections to scalar QED,” *Phys. Rev. D* **66** (2002), 084023 [arXiv:hep-th/0206236 [hep-th]].
- [40] N. E. J. Bjerrum-Bohr, J. F. Donoghue and B. R. Holstein, “Quantum gravitational corrections to the nonrelativistic scattering potential of two masses,” *Phys. Rev. D* **67** (2003), 084033 [erratum: *Phys. Rev. D* **71** (2005), 069903] [arXiv:hep-th/0211072 [hep-th]].
- [41] H. Lehmann, K. Symanzik and W. Zimmermann, “On the formulation of quantized field theories,” *Nuovo Cim.* **1** (1955), 205-225
- [42] D. Marolf, I. A. Morrison and M. Srednicki, “Perturbative S-matrix for massive scalar fields in global de Sitter space,” *Class. Quant. Grav.* **30**, 155023 (2013) [arXiv:1209.6039 [hep-th]].
- [43] S. Melville and G. L. Pimentel, “de Sitter S matrix for the masses,” *Phys. Rev. D* **110** (2024) no.10, 103530 [arXiv:2309.07092 [hep-th]].
- [44] S. Melville and G. L. Pimentel, “A de Sitter S-matrix from amputated cosmological correlators,” *JHEP* **08** (2024), 211 [arXiv:2404.05712 [hep-th]].

- [45] J. F. Donoghue and T. Torma, “On the power counting of loop diagrams in general relativity,” *Phys. Rev. D* **54** (1996), 4963-4972 [arXiv:hep-th/9602121 [hep-th]].
- [46] S. Katuwal and R. P. Woodard, “Gauge independent quantum gravitational corrections to Maxwell’s equation,” *JHEP* **10** (2021), 029 [arXiv:2107.13341 [gr-qc]].
- [47] D. Glavan, S. P. Miao, T. Prokopec and R. P. Woodard, “Graviton Propagator in a 2-Parameter Family of de Sitter Breaking Gauges,” *JHEP* **10** (2019), 096 [arXiv:1908.06064 [gr-qc]].
- [48] D. Glavan, “Graviton propagator in de Sitter space in a simple one-parameter gauge,” [arXiv:2511.13660 [gr-qc]].
- [49] D. Glavan, S. P. Miao, T. Prokopec and R. P. Woodard, “Gauge independent logarithms from inflationary gravitons,” *JHEP* **03** (2024), 129 [arXiv:2402.05452 [hep-th]].
- [50] J. M. Bardeen, “Gauge Invariant Cosmological Perturbations,” *Phys. Rev. D* **22**, 1882-1905 (1980)
- [51] N. C. Tsamis and R. P. Woodard, “Physical Green’s Functions in Quantum Gravity,” *Annals Phys.* **215**, 96-155 (1992)
- [52] S. Carlip, “Quantum gravity: A Progress report,” *Rept. Prog. Phys.* **64**, 885 (2001) [arXiv:gr-qc/0108040 [gr-qc]].
- [53] L. R. Abramo and R. P. Woodard, “A Scalar measure of the local expansion rate,” *Phys. Rev. D* **65**, 043507 (2002) [arXiv:astro-ph/0109271 [astro-ph]].
- [54] G. Geshnizjani and R. Brandenberger, “Back reaction and local cosmological expansion rate,” *Phys. Rev. D* **66**, 123507 (2002) [arXiv:gr-qc/0204074 [gr-qc]].
- [55] S. B. Giddings, D. Marolf and J. B. Hartle, “Observables in effective gravity,” *Phys. Rev. D* **74**, 064018 (2006) [arXiv:hep-th/0512200 [hep-th]].
- [56] T. Tanaka and Y. Urakawa, “Loops in inflationary correlation functions,” *Class. Quant. Grav.* **30**, 233001 (2013) [arXiv:1306.4461 [hep-th]].
- [57] W. Donnelly and S. B. Giddings, “Diffeomorphism-invariant observables and their nonlocal algebra,” *Phys. Rev. D* **93**, no.2, 024030 (2016) [erratum: *Phys. Rev. D* **94**, no.2, 029903 (2016)] [arXiv:1507.07921 [hep-th]].
- [58] I. Khavkine, “Local and gauge invariant observables in gravity,” *Class. Quant. Grav.* **32**, no.18, 185019 (2015) [arXiv:1503.03754 [gr-qc]].
- [59] D. Marolf, “Comments on Microcausality, Chaos, and Gravitational Observables,” *Class. Quant. Grav.* **32**, no.24, 245003 (2015) [arXiv:1508.00939 [gr-qc]].
- [60] M. B. Fröb, “Gauge-invariant quantum gravitational corrections to correlation functions,” *Class. Quant. Grav.* **35**, no.5, 055006 (2018) [arXiv:1710.00839 [gr-qc]].
- [61] M. B. Fröb and W. C. C. Lima, “Propagators for gauge-invariant observables in cosmology,” *Class. Quant. Grav.* **35**, no.9, 095010 (2018) [arXiv:1711.08470 [gr-qc]].
- [62] C. G. Torre, “Gravitational observables and local symmetries,” *Phys. Rev. D* **48**, R2373-R2376 (1993) [arXiv:gr-qc/9306030 [gr-qc]].
- [63] S. P. Miao and R. P. Woodard, “Issues Concerning Loop Corrections to the Primordial Power Spectra,” *JCAP* **07**, 008 (2012) [arXiv:1204.1784 [astro-ph.CO]].

- [64] S. P. Miao, N. C. Tsamis and R. P. Woodard, “Invariant measure of the one-loop quantum gravitational backreaction on inflation,” *Phys. Rev. D* **95**, no.12, 125008 (2017) [arXiv:1702.05694 [gr-qc]].
- [65] M. B. Fröb, “One-loop quantum gravitational corrections to the scalar two-point function at fixed geodesic distance,” *Class. Quant. Grav.* **35**, no.3, 035005 (2018) [arXiv:1706.01891 [hep-th]].
- [66] N. N. Bogoliubov and O. S. Parasiuk, “On the Multiplication of the causal function in the quantum theory of fields,” *Acta Math.* **97**, 227-266 (1957)
- [67] K. Hepp, “Proof of the Bogolyubov-Parasiuk theorem on renormalization,” *Commun. Math. Phys.* **2**, 301-326 (1966)
- [68] W. Zimmermann, “The power counting theorem for minkowski metric,” *Commun. Math. Phys.* **11**, 1-8 (1968)
- [69] W. Zimmermann, “Convergence of Bogolyubov’s method of renormalization in momentum space,” *Commun. Math. Phys.* **15**, 208-234 (1969)
- [70] C. Itzykson and J. B. Zuber, “Quantum Field Theory,” McGraw-Hill, 1980, ISBN 978-0-486-44568-7
- [71] S. Weinberg, “The quantum theory of fields. Vol. 2: Modern applications,” Cambridge University Press, 2013, ISBN 978-1-139-63247-8, 978-0-521-67054-8, 978-0-521-55002-4
- [72] G. P. Korchemsky and A. V. Radyushkin, “Renormalization of the Wilson Loops Beyond the Leading Order,” *Nucl. Phys. B* **283**, 342-364 (1987)
- [73] E. T. Akhmedov, A. Roura and A. Sadofyev, “Classical radiation by free-falling charges in de Sitter spacetime,” *Phys. Rev. D* **82** (2010), 044035 [arXiv:1006.3274 [gr-qc]].
- [74] D. Glavan, S. P. Miao, T. Prokopec and R. P. Woodard, “Breaking of scaling symmetry by massless scalar on de Sitter,” *Phys. Lett. B* **798** (2019), 134944 [arXiv:1908.11113 [gr-qc]].
- [75] J. S. Schwinger, “Brownian motion of a quantum oscillator,” *J. Math. Phys.* **2** (1961), 407-432
- [76] K. T. Mahanthappa, “Multiple production of photons in quantum electrodynamics,” *Phys. Rev.* **126** (1962), 329-340
- [77] P. M. Bakshi and K. T. Mahanthappa, “Expectation value formalism in quantum field theory. 1.,” *J. Math. Phys.* **4** (1963), 1-11
- [78] P. M. Bakshi and K. T. Mahanthappa, “Expectation value formalism in quantum field theory. 2.,” *J. Math. Phys.* **4** (1963), 12-16
- [79] L. V. Keldysh, “Diagram Technique for Nonequilibrium Processes,” *Sov. Phys. JETP* **20** (1965), 1018-1026
- [80] K. c. Chou, Z. b. Su, B. l. Hao and L. Yu, “Equilibrium and Nonequilibrium Formalisms Made Unified,” *Phys. Rept.* **118** (1985), 1-131
- [81] R. D. Jordan, “Effective Field Equations for Expectation Values,” *Phys. Rev. D* **33** (1986), 444-454
- [82] L. H. Ford and R. P. Woodard, “Stress tensor correlators in the Schwinger-Keldysh formalism,” *Class. Quant. Grav.* **22** (2005), 1637-1647 [arXiv:gr-qc/0411003 [gr-qc]].

- [83] N. A. Chernikov and E. A. Tagirov, “Quantum theory of scalar field in de Sitter space-time,” *Ann. Inst. H. Poincare Phys. Theor. A* **9** (1968) no.2, 109-141
- [84] B. Allen and A. Folacci, “The Massless Minimally Coupled Scalar Field in De Sitter Space,” *Phys. Rev. D* **35** (1987), 3771
- [85] V. K. Onemli and R. P. Woodard, “Superacceleration from massless, minimally coupled ϕ^4 ,” *Class. Quant. Grav.* **19** (2002), 4607 [arXiv:gr-qc/0204065 [gr-qc]].
- [86] T. M. Janssen, S. P. Miao, T. Prokopec and R. P. Woodard, “Infrared Propagator Corrections for Constant Deceleration,” *Class. Quant. Grav.* **25** (2008), 245013 [arXiv:0808.2449 [gr-qc]].
- [87] S. P. Miao, N. C. Tsamis and R. P. Woodard, “The Graviton Propagator in de Donder Gauge on de Sitter Background,” *J. Math. Phys.* **52** (2011), 122301 [arXiv:1106.0925 [gr-qc]].